CHALMERS
UNIVERSITY OF TECHNOLOGY

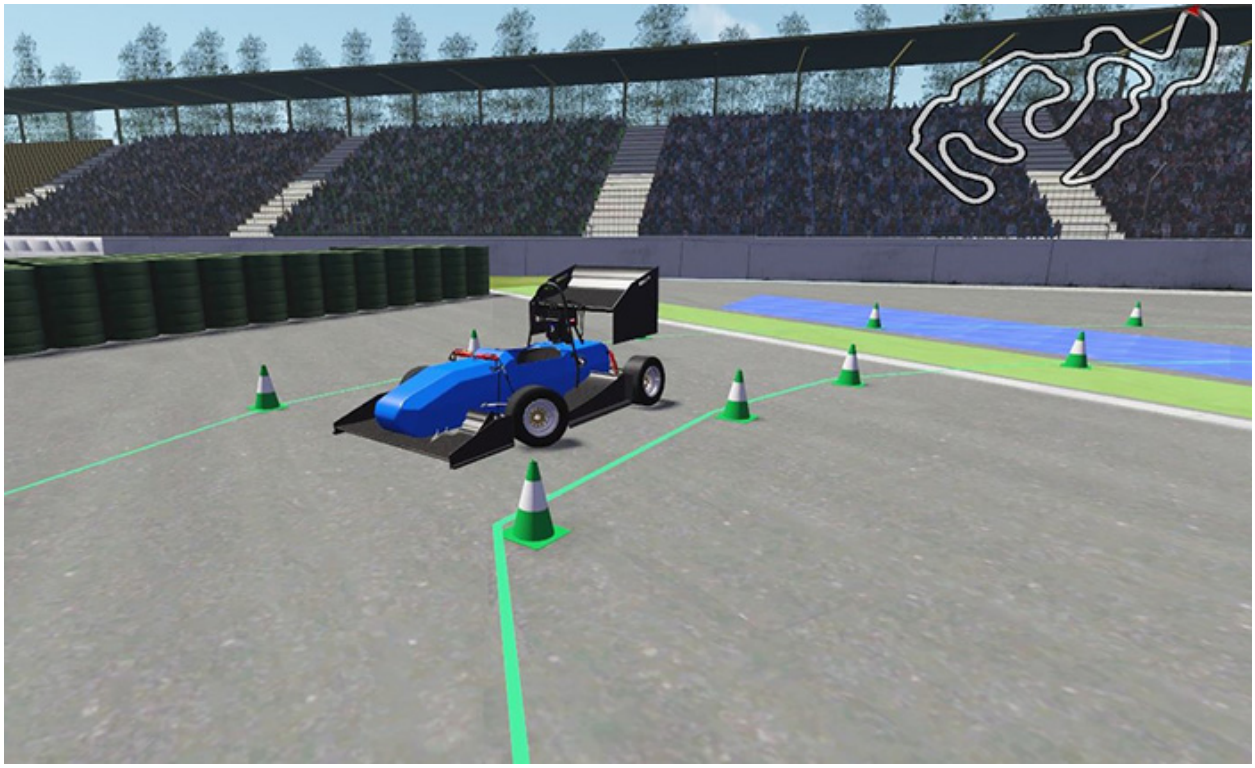

Modelling and Validation of a Dynamic Vehicle Model for use in a Motion Based Simulator

Bachelor's thesis in Mechanical Engineering

Richard Löfwenberg

Kristian Ivancic

Eric Gunnarsson

Mechanics and Maritime Sciences
CHALMERS UNIVERSITY OF TECHNOLOGY
Gothenburg, Sweden 2018

Bachelor's thesis 2018:27

MMSX20-18-09 Modelling and Validation of a Dynamic Vehicle Model for use in a Motion Based Simulator

Richard Löfwenberg
Kristian Ivancic
Eric Gunnarsson

CHALMERS
UNIVERSITY OF TECHNOLOGY

Department of Mechanics and Maritime Sciences
Division of Vehicle Engineering and Autonomous Systems
Vehicle Dynamics group
Chalmers University of Technology
Gothenburg, Sweden 2018

Modelling and Validation of a Dynamic Vehicle Model for use in a Motion Based Simulator
Richard Löfwenberg, Kristian Ivancic, Eric Gunnarsson

Supervisor: Ingemar Johansson, CEVT and Vehicle Engineering and Autonomous Systems
Examiner: Bengt Jacobson, Vehicle Dynamics at Vehicle Engineering and Autonomous Systems

Bachelor's Thesis 2018:27
Department of Mechanics and Maritime Sciences
Division of Vehicle Engineering and Autonomous Systems
Vehicle Dynamics group
Chalmers University of Technology
SE-412 96 Gothenburg
Telephone +46 31 772 1000

Cover: Chalmers Formula Student car in the simulation environment.

Typeset in LaTeX
Gothenburg, Sweden 2018

Modelling and Validation of a Dynamic Vehicle Model for use in a Motion Based Simulator
Richard Löfwenberg, Kristian Ivancic, Eric Gunnarsson
Department of Mechanics and Maritime Sciences
Chalmers University of Technology

Abstract

The increase in computational power in recent years has enabled advanced driving simulations. This has allowed engineers to make informed decisions during early design phases. In motorsport applications, simulators are widely used for drivers practice. This thesis describes a method of how to translate vehicle data to parameters used in the motion based driving simulator at Chalmers University of Technology. This was done by modeling the Chalmers Formula Student 2017 car and implementing it into the simulating software Panthera. Furthermore the implemented model was tuned and validated by objective metrics as well as subjective assessments.

Keywords: simulator, motorsport, modeling, vehicle dynamics, validation, handling, tire modeling, suspension, kinematics

Acknowledgements

This thesis would not have been possible without the help from our supervisor and mentor Ingemar Johansson, who has provided us with guidance, knowledge and understanding. We would also like to give a special thanks to Bengt Jacobsson, for his support as examiner of the project. A big thanks to Chalmers Formula Student for providing us with their data and support. Having the opportunity to work with Axel Niklasson as driver offered an outstanding way to evaluate the vehicle model and discuss subjective assessments. Finally, we would like to thank Caster, who gave us access to their facility and use of the simulator.

Richard Löfwenberg, Kristian Ivancic, Eric Gunnarsson, Gothenburg, May 2018

Notations

AoA	Angle of Attack	The angle of a generic airfoil from the x-y-plane.
ARB	Anti Roll Bar	Flexible bar connecting the wheels of an axle
CAD	Computer Aided Design	Term describing the use of computers when designing
CAE	Computer Aided Engineering	Term describing the use of computers in engineering, such as 3D-modelling and large computations
CFS	Chalmers Formula Student	Project at Chalmers that participates in Formula Student.
CFS17	Chalmers Formula Student 2017	The 2017 Chalmers Formula Student team.
CoG	Center of Gravity	Refers to the mass center of the car
CoP	Center of Pressure	Refers to a point on the car where aerodynamic forces are acting.
DIL	Driver In the Loop	Term describing when a human driver is in the loop as part of the simulation of a vehicle.
FSG	Formula Student Germany	The Formula Student competition that takes place in Germany
FSGE	Formula Student Germany Endurance	The FSG endurance event
K&C	Kinematic and Compliance	Kinematic refers to how the suspension moves due to the geometries, that is if all links where rigid and joints moment free. Compliance refers to how the suspension moves due to bushings and flexibility of links and fixation points.
LSD	Limited Slip Differential	A type of differential.
RMS	Root Mean Square	Measure of the spread of deviation
TV	Torque Vectoring	Term describing the controlling of torque distributed on an axle.
UDP	User Datagram Protocol	A communication protocol used by computers over the internet.

Contents

1
Introduction

1.1 Background

In an ever changing car industry with a growing competition for market shares, the time dedicated for development of a new car model is constantly being shortened. This demands continuous improvements regarding concept development and evaluation in early phases of projects. Together with the increase of computational power in computers this has laid a foundation for a CAE-based development phase. To achieve the desired vehicle dynamic behaviour in an early project phase, there is a growing interest in the possibilities of motion based DIL-simulators. One of the suppliers of such systems is Cruden. The simulator at Chalmers University of Technology uses a system supplied by Cruden.

1.2 Problem description

While vehicles are often developed using different simulating tools, they are not always corresponding to the real vehicle in question. As the industry is implementing increasingly advanced simulating tools to assess the subjective behaviour of a vehicle model, there is a need for simulation models with high fidelity in both objective metrics and subjective assessments. The Panthera system used in the Cruden simulator has a built in parameter based vehicle model. Although vehicles has earlier been implemented, it has not been done thoroughly at Chalmers.

1.3 Objective

The aim of this bachelor thesis is to describe the process of modelling a vehicle for use in the DIL-simulator at Chalmers. The objective is likewise to deliver a vehicle model, validated by a given set of objective metrics and subjective assessments.

1.4 Deliverables

The thesis will deliver a process of how to:

- Derive parameter values for Panthera using suspension design data.
- Derive parameter values for Panthera using simulated K&C-test data.
- Derive parameter values for Panthera using spec data.

- Derive parameter values for Panthera using logged data.
- Derive parameter values for Panthera using raw tire data.
- Validate the parameter values using objective metrics by logged racing-data.
- Validate the parameter values through subjective assessment in the simulator by an experienced racing driver.
- Tune the parameter values through subjective assessment in the simulator by an experienced racing driver.

The thesis will also deliver:

- A validated and implemented vehicle model in the Caster simulator.

1.5 Limitations

- The project will use Panthera as real time simulation software.
- Implementation of graphics and audio is to be kept at minimum.
- Only dry weather conditions will be considered when simulating the vehicle.
- Main modeling focus will be put on suspension and tires.
- Torque vectoring will not be modeled.

2

Scope

2.1 Vehicle

The vehicle that will be modeled is the Chalmers Formula Student 2017 car. This is an open wheel race car that was used in Formula Student competitions during the summer of 2017. It is an electric car with two individual motors, one for each rear wheel.

Figure 2.1: Chalmers Formula Student 2017 car

The main reasons for modeling the CFS17 are summarized in the table shown below.

- Full access to detailed engineering data
- Full access to all logged data both from testing and the competitions
- Access to drivers both with experience from the simulator and driving the car in real life
- Possibility to talk with the engineers who built the car
- The car has a very stiff chassis with very few bushings, reducing the error level
- There is an expressed need from the CFS team, of a vehicle model to be used for drivers training

2.2 Simulator

The simulator used is a model called Hexatech 1CTR by the manufacturer Cruden. It uses six actuators to simulate motion from the vehicle model. From the drivers perspective there is a steering wheel, three foot pedals and a dashboard. For shifting there is the choice between paddles and a gear stick. The steering wheel has force feedback with a max torque of 30 Nm enabling high steering wheel torque thus possibility of providing a correct steering feel. Motion cuing parameters are tuneable in the filter between the vehicle model and platform motion.

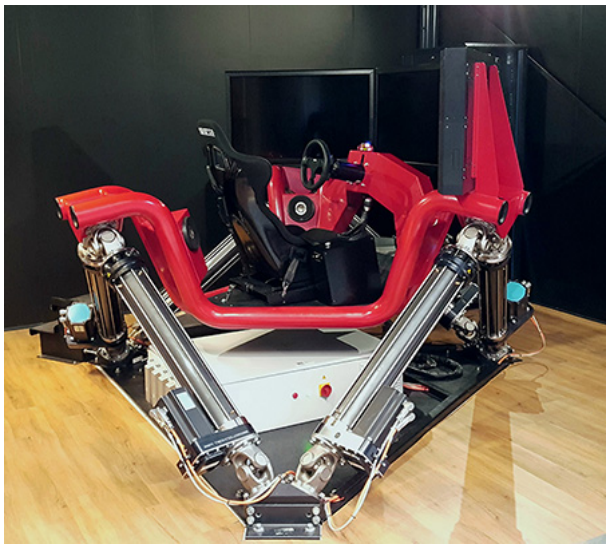

Figure 2.2: Hexatech 1CTR at Caster

2.3 Panthera

Panthera is the simulating software developed by Cruden. It runs the physics and graphics engine as well as communicating with the motion based platform [2]. It's used for real time simulations in DIL-simulators. This thesis will be using the built in vehicle model in Panthera which is defined by a set of parameters. These parameters are defined in the so called *car.ini* file. The internal model was chosen since it was considered to be robust. The parameters used in the vehicle model can be categorized in to the following groups:

- Body and Aero
- Engine and Drivetrain
- Suspension and Steering
- Wheels and Tires

Figure 2.3: Caster formula car in Panthera

Being an already built and compiled vehicle model it has some limitations:

- The model is simplified in many areas, only allowing linear behaviour of geometry effects.
- The model is limited in the inputs, there is limited to no support to control the model with for example Matlab, limiting the possibility of offline testing.
- For the same reason as above, implementation of active systems such as torque vectoring is limited.

2.4 Dymola and VDL

Dymola is a widely used multipurpose simulation software based on the Modelica language. VDL refers to the Vehicle Dynamics Library in Dymola, developed by the company Modelon. This is a package with various templates of models often used in vehicle dynamics simulations. It also has an extensive amount of template test rigs, for example the possibility to simulate K&C-tests.

3
Theory

3.1 Simulation

The word simulation originates from the latin word for mimic or pretend, si'mulo. It is a word to describe the way of playing out an event without it actually happening. It can be fully computational or partly played out in reality in a controlled manner, for example a wind tunnel experiment. [3]

3.1.1 Simulator

Simulator is the word for an **object** used to simulate a certain event. A simulator can be used for practice, entertainment or development. In the automotive industry, simulators are often used to visualize and supply the user with a subjective experience of the product under development. [4]

3.1.2 Human perception in a simulator

The goal of a DIL-simulator is to mimic the actual experience to its fullest. This can be done by deceiving the human senses in different ways. A motion based simulator uses its actuators to move the platform in order to affect the human vestibular system to register movements in the way the real event would play out. The steering wheel simulates the actual steering feel. The screens shows moving images and the speakers plays a simulated sound, all to enhance the virtual experience.

3.2 Tires

To understand the dynamics of a vehicle one has to realize the importance of tires. In a properly designed vehicle, tires are the only thing touching the ground, where the largest forces on the body are generated through the contact patch of the tires. The tire forces on the steered axle are fed through the steering mechanism and can be felt through the steering wheel. Tires supply traction, braking and lateral forces for controlling and stabilizing the vehicle. With this in mind it becomes clear that the tires are of great importance for the performance and perception of a vehicle.

Tires, in this case, refers to pneumatic tires. During the last 40 years there has been major advances in knowledge regarding the manufacturing and behaviour of pneumatic tires. For this project, models known as Magic Formulas were used. This in order to model the tires as well as to make data driven decisions and estimations of the tire behaviour.

3.2.1 Longitudinal Properties

The first detail to consider when analyzing tire behaviour is the fact that the tire is elastic and that it is constantly deflecting. For example this affects the tire radius when a vertical load is applied and further so when torque is acting on the wheel. The tire can not be seen as a direct link between translational- and angular velocity since the rolling radius will give rise to a different translational velocity compared to the unloaded radius.

The elastic properties of a pneumatic tire will give rise to what is referred to as rolling resistance. SS-ISO defines it as a force derived from the loss of energy in the tire per unit distance[5]. It is a phenomena occurring as a result of multiple factors, though the main contribution when considering an arbitrary wheel of a moving vehicle is that the pressure distribution is bigger and located towards the leading "edge" of the wheel. This is a consequence of the pressure distribution as well as damping and velocity effects. Due to shear of the tire walls the contact patch will also move towards the leading edge of the tire. As a result of this the reaction force from the road to the tire will be located with an offset from the wheel center causing an opposing torque. The rolling resistance is then in fact a torque loss which is to be subtracted from the propulsion torque[6]. With this in mind, the rolling resistance is not to be referred to, or taken as rolling friction. What is often used to describe the losses of torque as a result of rolling resistance is the rolling coefficient. The rolling coefficient is according to the same standard, SS-ISO, defined as the ratio of the tire rolling resistance force to the tire normal force. To mention is also the fact that the rolling moment among other things changes with ground surface, temperature, tire pressure and compound.

When looking at longitudinal forces produced by the tire, tests and experiments have shown that the friction force of the pneumatic tire initially gives rise to a linear region. As the slip increases so does the longitudinal force up to a point where it

reaches its maximum value. After this point the tire saturates and does not produce additional longitudinal friction force. All tires do not have this peak value, but it is commonly seen among racing tires.

3.2.2 Lateral Properties

The elasticity of the pneumatic tire has already been mentioned in section 3.2.1 and will also have a substantial effect on the lateral properties of the tire. When steering the vehicle, the orientation of the tire changes. As mentioned in [7], the proportion of the tread in contact with the road will resist the turning moment due to the elastic friction between the rubber and the road and will then not turn as far as the actual wheel, giving rise to an angular displacement in the direction the tire is moving and the path it is actually following. This displacement is referred to as the slip angle.

Since the coefficient of friction naturally changes with the degree of slip angle, so does the lateral force produced by the tire. This lateral force will increase with added slip angle up to a point where it reaches its peak value. The peak slip angle is the maximum value of the tire lateral force at a certain friction coefficient attainable on a specified surface, under a given set of operating conditions [5]. When considering empirical tire models, the lateral force initially increases linearly with the slip angle up to a point after which the stiffness starts to decrease with the slope of the curve. This non linear region will then lead up to a peak slip angle value at which the maximum tire cornering force is reached. After this point one can expect the cornering force to decrease.

The tire performance changes with the amount of vertical load on the tire, which is a clear result of the cornering stiffness changing with variations in vertical load. There are several reasons for the decrease in cornering stiffness with added load. For example as mentioned in [6] one cause is the result of nonuniform pressure distribution and contact patch length variation. For the understanding of this report one does not need to fully understand the underlying process of why the cornering stiffness actually is showing a degressive characteristic. The understanding of its influence on tire performance is considered more important.

The tire shear stress will be concentrated at a rearward and outboard position from the wheel rotating axis and wheel centre line. Since this is the point through which the side force will be generated the pneumatic trail defined by the offset distance will act as a moment arm and will result in a resistance to turning the wheel. This resistance then contributes to the self aligning torque but as opposed to caster and scrub radius covered in section 3.3.4, it varies more rapidly with slip angle. To mention is also that since the tire during cornering deflects laterally from the centre line, the normal force will act at an offset position resulting in an overturning moment which is enhanced by the lateral force. [6, 7]

The camber angle described in section 3.3.4, affects both the longitudinal and lateral performance of the tire. With the tire operating at an angle, the tire contact patch area is affected. When considering tires it must be kept in mind that the area of contact is dependent on the normal load of the tire [8], which increases with added load. As mentioned in [6] one component of the tire grip is due to adhesion. In order for this component to be as big as possible the tire has to be in close contact with the road. Higher normal loads will then force the tire to form with the road irregularities allowing for more adhesion. It can then be argued that the longitudinal tire grip will decrease with increased camber angle since one side of the wheel is moved upwards. Due to the limitations of this thesis, this is not further analyzed, though it may play an important role in tire modeling. Laterally camber has a positive affect contributing to was is called camber thrust. As tire tread approaches the leading edge of the contact patch it gets forced to travel in a straight line instead of following the natural path of the tire circumference. This deformation gives rise to camber thrust and enhances the lateral force. [7, 8, 9]

3.2.3 Combined Properties

Since the vehicle is mostly operating in a combination of lateral and longitudinal forces there is a need to express the performance of the tire under these combined conditions. This can be done with the friction ellipse shown in figure C.4.

3.2.4 Magic Formulas

Magic Formulas are used for modeling tire behaviour, which is done through curve fitting of tire raw data. This report will not elaborate on the way this is done. The understanding of the obtained information from these models is considered more important for the purpose of this report. Some examples of magic formulas are the Pacejka 89 and Pacejka 96 formulas developed by Hans B. Pacejka. Due to a misunderstanding during the development of Panthera, it sometimes refers to the Pacejka 96, while it actually uses the Pacejka 89. Another example of a magic formula is MF 5.2. The potential of using this model is discussed in section 4.8. [10]

3.3 Suspension

Vehicles need to operate under a big range of conditions in a safe way, providing the driver with the information needed. Through the years engineers have gathered knowledge in how a suspension should be designed for the corresponding application.

3.3.1 Suspension components

A suspension is usually designed with a number of standard components. The ones used on the CFS17 car are described in this section.

Springs are crucial parts in defining the characteristics of the vehicle. They are used to control the movement of the wheel and to even out disturbances from the road[11].

Dampers are used to reduce energy and to dampen vibrations in the suspension system[11].

Control arms and **link arms** connects the wheel to the vehicle structure.

Upright connects the wheel and the control arms.

Pull rods connects the rocker to the upper part of the upright.

Rocker connects the pull rod to the spring and damper.

Anti-roll bar connects the two wheels on the same axle with a torsion bar. This transfers deflection from one side to the other side and thus increasing roll stiffness.

3.3.2 Suspension types

There is a variety of different suspension types. The choice of suspension type depends on the specific vehicle and its conditions of operation. Because of the muchness of suspension types, this section will only cover the suspension used in the CFS17 car, a double wishbone pull rod suspension with rocker arms.

Double wishbone suspension is based on control arms, shaped like a-arms, which each has three attachment points, two at the chassis and one at the upright. This is a setup where a large amount of behaviours can be achieved just by having links with different lengths. Rather than connecting the spring to a control arm as is common in a normal wishbone suspension, the CFS17 car uses a pull rod and rocker setup. The pull rod actuates the rocker, where the spring, damper and ARB is attached. This creates a greater freedom in setting the motion ratio and possibility to relocate the springs and dampers.

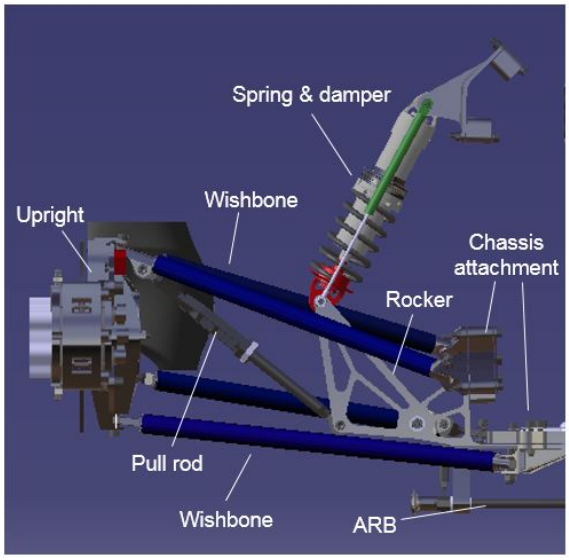

Figure 3.1: Rear suspension, courtesy of CFS

3.3.3 Suspension geometry

A suspension is defined by its geometry, some of these geometries are introduced in this section.

Hard points are the coordinates where the different attachments in a suspension is placed with relation to a determined null-point. Figure 3.2 shows some examples of hard points.

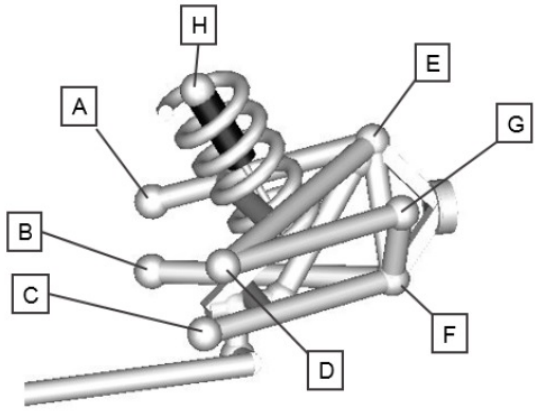

A - For upper chassis attachment.
B - For lower chassis attachment.
C - Aft lower chassis attachment.
D - Aft upper chassis attachment.
E - Upper hub attachment.
F - Lower hub attachment.
G - Toe-link hub attachment.
H - Spring and damper chassis attachment.

Figure 3.2: Hardpoints

Motion ratio is the ratio between the actuation of the wheel and the spring and damper. In a suspension where the spring is attached to the lower wishbone this ratio is normally around 0.7, according to Ingemar Johansson, professor of the practice, Chalmers.

Ackermann is the difference in steering angle on the inner and outer wheel. It is given as a ratio where 1 is full Ackermann and 0 is parallel steer [5]. Panthera uses another definition. Here it is defined as the how much more the inner wheel will turn than the outer wheel, where a value of 1 means parallel steer [10].

Anti-pitch is a geometrical property of the suspension that counteracts pitch of the body during braking and acceleration[11]. It is explained thoroughly in [12, Chapter 10].

Roll-center is defined as the point of intersection between the lines from the contact patches to the suspension pivot center, in the y-z-plane. This is usually, at a stationary position, in coincidence with the vehicle center line, see figure 3.3. [11]

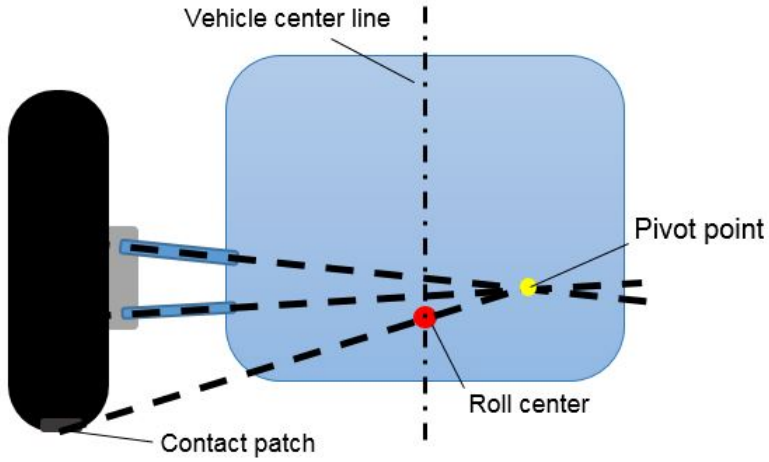

Figure 3.3: Roll center

Steer jacking is the phenomena that the wheel will lift or lower as an effect of the steering angle[12].

3.3.4 Wheel orientation

To secure a steady and secure ride with the correct handling the wheel orientation is designed in a certain way. As seen in figure 3.4 and the wheel has different angles and offsets which will affect the vehicle suspension. Unless other specified, the explanations below are according to SS-ISO[5].

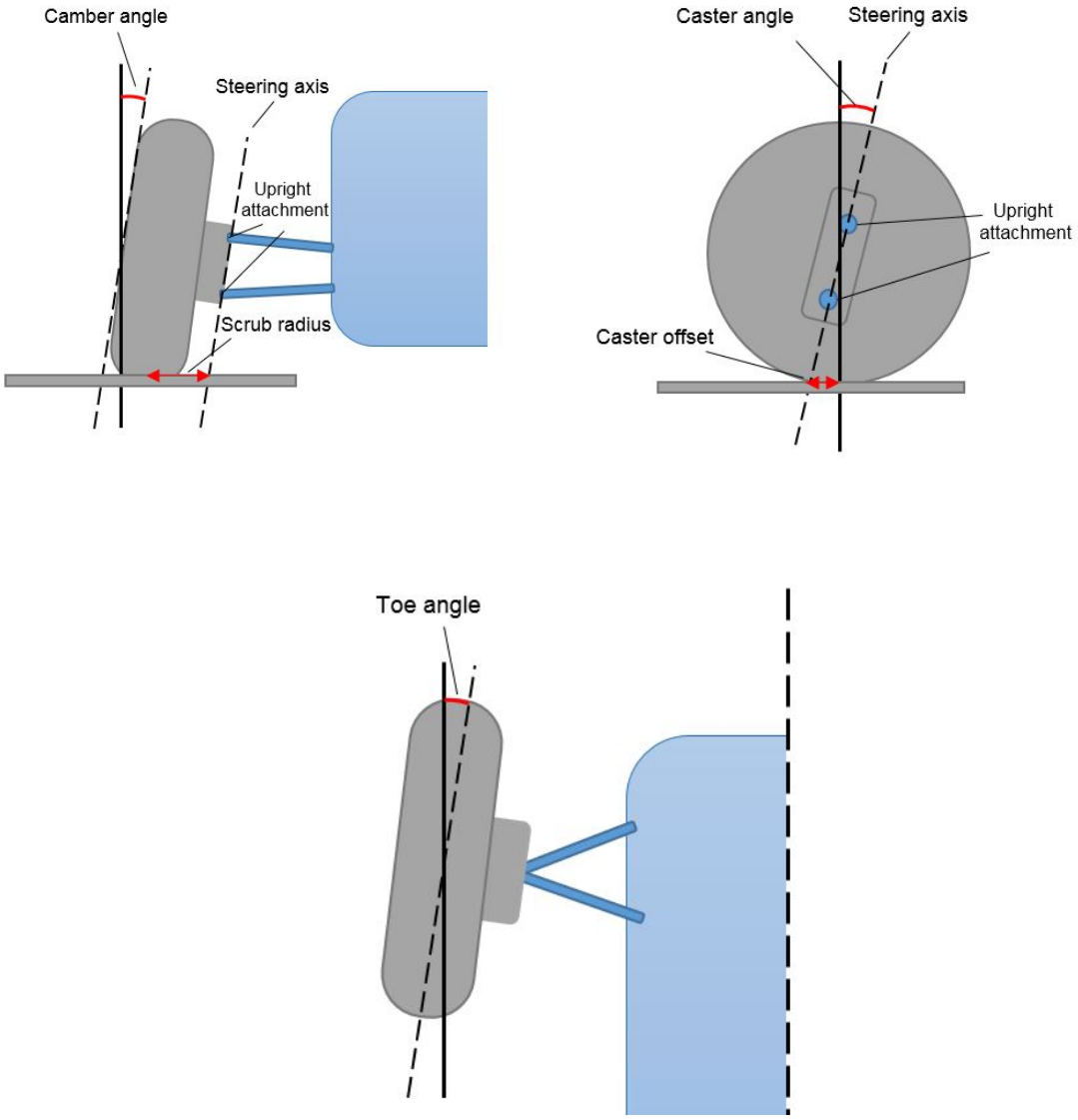

Figure 3.4: Wheel orientations

Camber angle is the offset-angle towards a vertical line through the wheel center seen in the y-z plane. It is positive if the top of the wheel is pointing away from the vehicle and negative if its pointing towards the vehicle. When the wheel is deflected up or down the suspension will usually cause camber to change. This is called **bump camber**.

Toe angle is the offset angle between the wheel and x-axis when the steering wheel is in a straight ahead position. Toe is affected by wheel deflection causing the toe angle to change. This is called **bump steer**.

Steering axis or kingpin axis is the axis that the wheel is rotating around when steering. When the vehicle has a double a-arm suspension this is defined by upper and lower upright attachment points.

Caster angle is the steering axis angle seen from the side of the wheel. The caster angle is positive when the top of the steering axis is inclined rearward.

Caster offset at ground is the distance from the intersection of the steering axle and the ground and the wheel center position at ground. As the tire forces are affecting the tire contact patch the caster offset at ground will work as a lever and create an aligning moment[11].

Kingpin angle is the steering axis angle seen from the rear of the wheel. Kingpin angle is positive when the top of the axis is inclined inward.

Scrub radius is the length from the intersection of the steering axis at ground to wheel center position at ground. Scrub radius affects steering moment as it creates a lever from contact patch to steering axis, thus the tire forces will create a moment[11].

3.4 Coordinate systems

Panthera uses the standard coordinate system for OpenGL(Open Graphics Library). It is defined as shown in figure 3.5a. This is different to the SS-ISO standard system which is defined as shown in figure 3.5b. [10, 5]

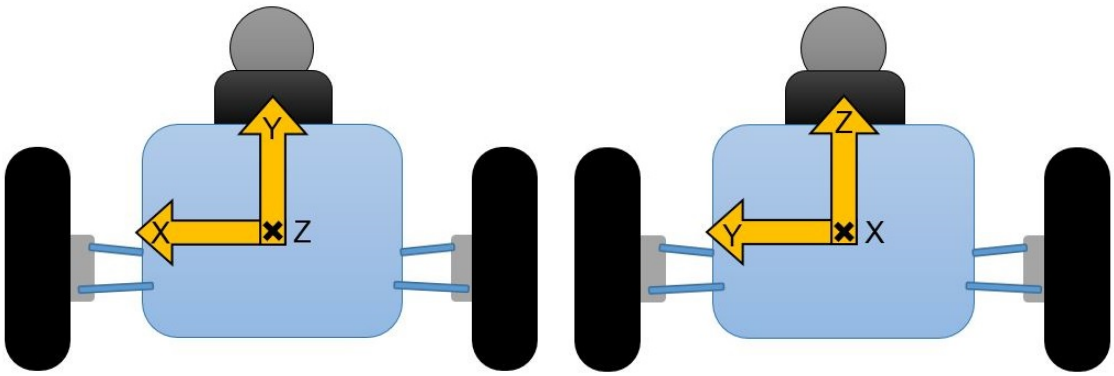

(a) OpenGL coordinate system **(b)** SS-ISO coordinate system

Figure 3.5: Coordination systems seen from behind a generic vehicle

3.5 Aerodynamics

Aerodynamic forces and moments that act upon a vehicle are often defined by a coefficient, C_f, and C_m respectively, presented in equation (3.1) where F is force, M is moment, ρ is air density, v is velocity, A is a reference area and l is a reference length.[11]

$$C_f = \frac{F}{\frac{1}{2}\rho v^2 A} \qquad C_m = \frac{M}{\frac{1}{2}\rho v^2 A l} \tag{3.1}$$

For a vehicle in a three dimensional space there are three body forces (lift, drag and side) and three body moments (pitch, roll and yaw) acting. Most vehicle bodies are symmetrical about the x-axis. In this case the number of forces and moments is reduced to three, the lift, drag and pitch. The pitch moment can be defined as a lift force acting on a specific point, the CoP, which then can be added by the body lift force defined by equation (3.2). Here L refers to the length from the CoP to the point where the pitch moment is defined(usually CoG).

$$F_{L,CoP} = F_L + M_p \cdot L \tag{3.2}$$

4
Development of method

4.1 Body and aerodynamics parameters

This section describes how the body and aerodynamics parameters was retrieved and implemented.

4.1.1 Mass and inertia

The body mass of the car was obtained by the full car assembly CAD file provided by CFS. In Panthera the body mass is defined as the weight of the vehicle including the driver, but with the engine and unsprung mass subtracted. Engine mass can be defined separately, however it does not alter the overall weight distribution of the vehicle in Panthera. When considering the wheel mass parameter, it is defined as the total unsprung mass at each respective corner of the vehicle. The body inertia was obtained from the CAD file and is defined as the rotational inertia about each axis. Engine, transmission and wheel rotational inertia was computed in CAD. For the wheel, the rotational inertia of the rim, centre piece, washer, brake disc and tire was put together and summarized.

4.1.2 Aerodynamics

In Panthera, one can define a body drag and multiple wings with both drag and lift coefficients. As the values from CFS were given as an overall C_L and an overall C_D together with the frontal area, the decision was taken to only define one wing in Panthera. A wing in Panthera is defined by its span length, cord length, AoA (in degrees), C_{down} and C_{drag}. The formula to calculate lift force in Panthera is defined in equation (4.1).

$$F_{down} = \frac{1}{2} L_{span} \cdot L_{cord} \cdot C_{down} \cdot (AoA + AoA_{offset}) \cdot \rho \cdot v^2 \tag{4.1}$$

Here AoA is defined in radians. Also notice that Panthera uses a *down* coefficient as opposed to a *lift* coefficient. To transform the formula used in Panthera to the formula normally used in aerodynamics, the following equality applies:

$$A_{frontal} = L_{span} \cdot L_{cord} \cdot (AoA + AoA_{offset})$$

The easiest way to use this formula is to set $L_{span} = A_{frontal}$ and set all the other parameters to 1. Please notice that Panthera wants the input of AoA in degrees, but transforms it to radians when calculating, hence a value of $\frac{180}{\pi} \approx 57.3$ should be entered instead of 1.

4.2 Engine and driveline parameters

In Panthera the engine performance is given as a normalized torque curve, see figure 4.1, and a maximum torque. The torque curve was retrieved from CFS with maximum torque, and normalized to be used in Panthera. The distribution of torque was chosen to be modeled as a limited slip differential. As the CFS17 car only has one gear, the final drive ratio was set to be the same as for the planetary gearbox.

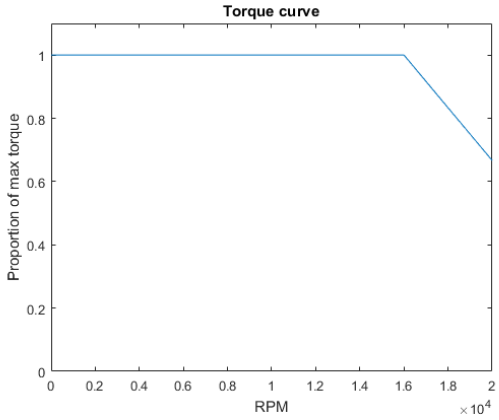

Figure 4.1: Torque curve

4.3 Modeling of suspension

As Panthera uses parameters that resembles the output from a kinematic analysis, a software capable of K&C-simulations was needed. The software chosen for this was Dymola 2018 together with the Vehicle Dynamics Library by Modelon. The modeling process started by choosing a resembling template for the suspension in question. The template accepts a set of hard points as input and can easily be changed to suit the suspension that is modelled. The hard points are defined with origin at the wheel hub.

4.3.1 Suspension set-up

In the VDL there are several templates for modeling vehicle suspensions. The template *FormulaTwinStrutSTT* was chosen for the front suspension and the corresponding template *FormulaTwinStrutTT* for the rear. Both templates have the same subsystems with the exception that the *FormulaTwinStrutTT* template does not have the steering system. The front suspension template with defined subsystems can be seen in figure 4.2.

The spring, dampers and compliance for the ARB are defined externally from the subsystem, as seen in figure 4.2. In the following sections, each subsystem will be elaborated with the exception of the subframe as it was chosen to be a rigid, massless system, which acts as a mounting point for the other subsystems.

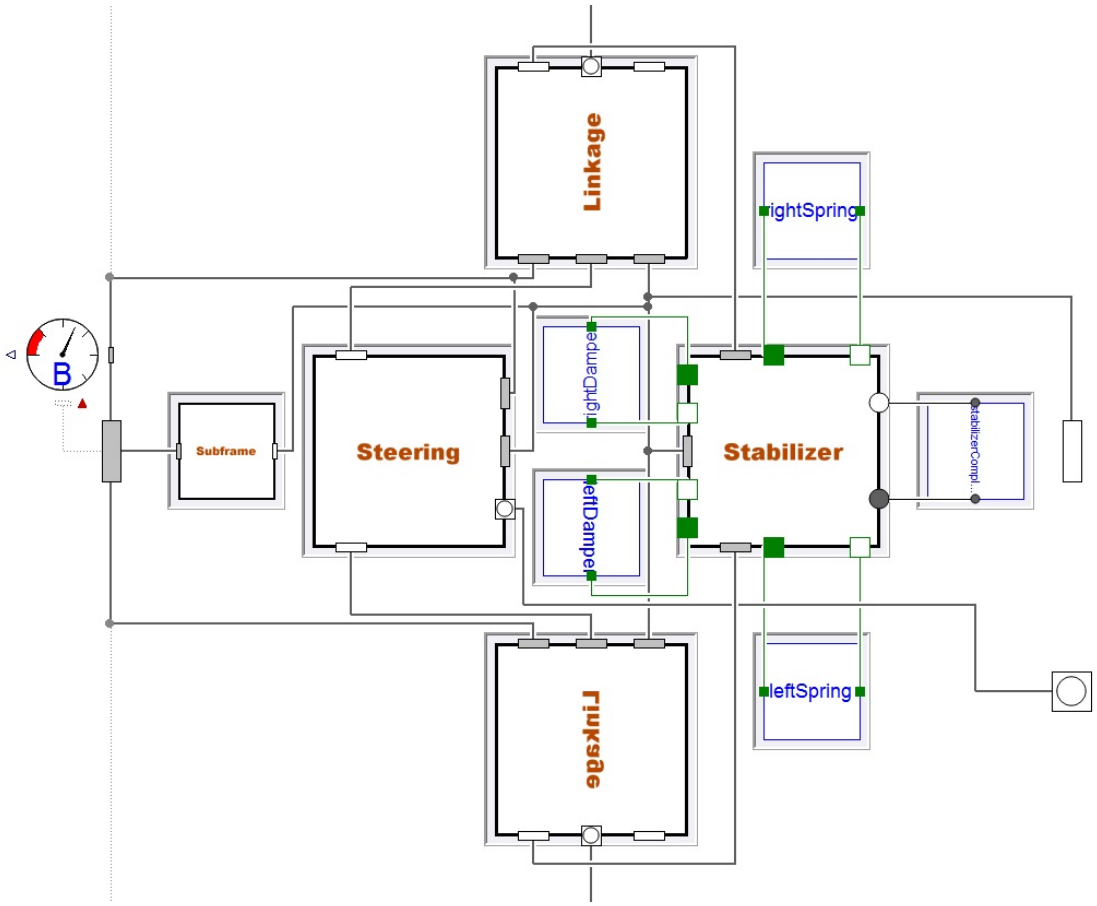

Figure 4.2: Template FormulaTwinStrutSTT

4.3.2 Linkage

The linkage subsections in the two suspension templates both have the same hard points, see figure 4.3. The difference is that for the rear suspension the steer linkage is the toe linkage.

Hard points

r0H	Position of hub center, resolved in vehicle frame
r0A	Position of origin of stabilizerFrame, resolved in vehicleFrame
r0CL1	Position of lower front link mount in chassis, resolved in vehicleFrame
r0CL2	Position of lower rear link mount in chassis, resolved in vehicleFrame
r0CL3	Position of upper front link mount in chassis, resolved in vehicleFrame
r0CL4	Position of upper rear link mount in chassis, resolved in vehicleFrame
r0CS	Position of spring mount in chassis, resolved in vehicleFrame
r0L1L2U	Position of lower spindle, resolved in vehicleFrame
r0L3L4U	Position of upper spindle, resolved in vehicleFrame
r0CL5	Position of steer link inner joint, resolved in vehicleFrame
r0L5U	Position of steer link outer joint, resolved in vehicleFrame

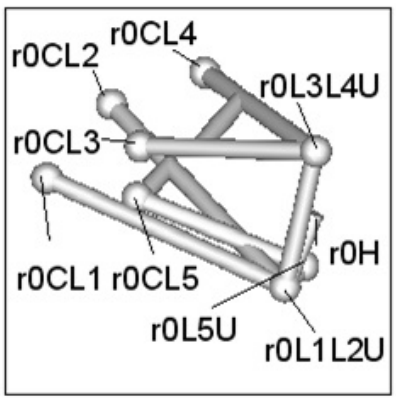

Figure 4.3: List of hard points for linkage subsystem

4.3.3 Stabilizer

The stabilizer used in *FormulaTwinStrutTT1* includes the rocker assembly with springs, damper and anti-roll bar. The template supports both push rod and pull rod suspension types, based on how the hard points are defined, see figure 4.4. Please note the typo for the last three hard points, saying right, all hard points shown in the figure applies to the left side.

Hard points

r0X_1	Position of leftFrameX, resolved in vehicleFrame
r0X_2	Position of rightFrameX, resolved in vehicleFrame
r0L1X_1	Position of outer end of left push/pull rod, resolved in vehicleFrame
r0L1P_1	Position of inner end of left push/pull rod at pivot element, resolved in vehicleFrame
r0CP_1	Position of left pivoting point, resolved in vehicleFrame
n0CP_1	Left pivoting axis
r0PS_1	Position of left spring mount in pivot element, resolved in vehicleFrame
r0DP_1	Position of left damper mount in pivot element, resolved in vehicleFrame
r0CS_1	Position of left spring mount in chassis, resolved in vehicleFrame
r0CD_1	Position of left damper mount in chassis, resolved in vehicleFrame
r0L2P_1	Position of right stabilizer link at pivot point, resolved in vehicleFrame
r0AL2_1	Position of right stabilizer link at lever, resolved in vehicleFrame
r0AC_1	Position of right stabilizer bar end to lever, resolved in vehicleFrame

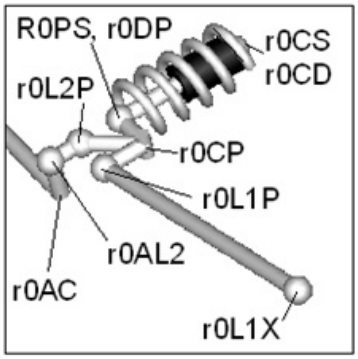

Figure 4.4: List of hard points for stabilizer subsystem

In the stabilizer, an additional stabilizer can be defined, the anti-roll bar. Here *IndependentAntiRollBar* was chosen. The anti-roll bar compliance was chosen as *Modelon.Mechanics.Rotational.LinearSpring*. This system uses a linear spring model defined in equation (4.2).

$$\text{torque} = c \cdot \text{angle} \tag{4.2}$$

This equation is based on a spring rate, c, with units of Nm/rad. Here the torsion is defined as the difference in torsion of each bar end. As the data supplied by CFS was defined by the roll of the whole vehicle, a spring rate had to be calculated by hand instead. The anti-roll bar is constructed in steel specially made for springs, with a E-module of 210 GPa, $\nu = 0.313$ and a diameter of 10 mm. The formula in equation (4.3) was used to calculate the spring rate. The length L is defined as the length between *r0AC_1*, from figure 4.4 and *r0AC_2* according to [13, p. 758] equation (21.7). This is an assumption that the bar only twists and doesn't bend and that the bar levers are completely stiff. This assumption was decided enough correct due to the construction of the anti-roll bar. The mounting points of the anti roll bar in the chassis is one of the few locations on the car that actually has bushings. These bushings are very stiff nylon bushings and were therefore neglected in these calculations.

$$c = \frac{E \cdot \pi \cdot d^4}{64 \cdot (1 + \nu) \cdot L} \tag{4.3}$$

As spring, a regular linear translational spring was used, *Modelon.Mechanics.Translational.LinearSpring*. In the CFS17 car a double spring setup is used, where one very soft support spring is mounted in series with the main spring. This setup

is used when the main spring is shorter than the actual travel of the suspension. When the suspension travel exceeds the length of the main spring, the support spring starts extending, making sure there is no play in the suspension. Under normal loads this support spring is completely compressed and can therefore be considered stiff. Due to the tight working range and time limitation, no effort was put into modeling this kind of springs and instead a regular spring was used. The damper data was supplied in a look-up table, matching velocity of travel with reaction force. Therefore *Modelon.Mechanics.Translational.TabularDamper* was used with linear interpolation between points.

4.3.4 Steering

For the steering, sub-system, *VehicleDynamics.Vehicles.Chassis.Suspensions.Steerings.Rack* was used. This is a basic rack and pinion steering without compliance. The hardpoints are defined in figure 4.5. *iPR* is defined as travel of the rack per radian of steering wheel rotation. The rack used is bought from the Canadian company Zedaro and is named *zRack 358*. As this is an off the shelf part, *iPR* could be found in the product specification.[14]

Hard points

r0R_1	Position of left rack end, resolved in vehicleFrame
r0R_2	Position of right rack end, resolved in vehicleFrame
r0PR	Position of pinion-rack center rotation center (gear wheel center), resolved in vehicleFrame
r0PZ	Position of lower steering column joint, resolved in vehicleFrame
r0QZ	Position of upper steering column joint, resolved in vehicleFrame
r0Q	Position of steering wheel center, resolved in vehicleFrame

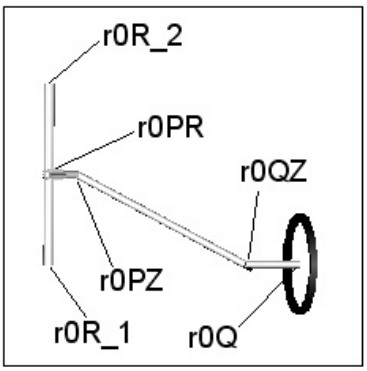

iPR	Ratio from pinion to rack (effective pinion radius) [m/rad]

Figure 4.5: List of hard points for steering subsystem

4.4 Generating kinematic data from suspension

To extract the data needed for Panthera, some kind of K&C-test was necessary. VDL has good K&C-rigs to simulate a test of this kind. K&C-simulations were done using simulation rigs included in VDL. For the front suspension, *SteerableSuspensionInRigKinematics* was used, shown in figure 4.6. For the rear, the corresponding *SuspensionInRigKinematics* was used. The rig is set up by including the suspension systems described in section 4.3.1 into the rig and then as a parameter to the controller defining which movements to simulate.

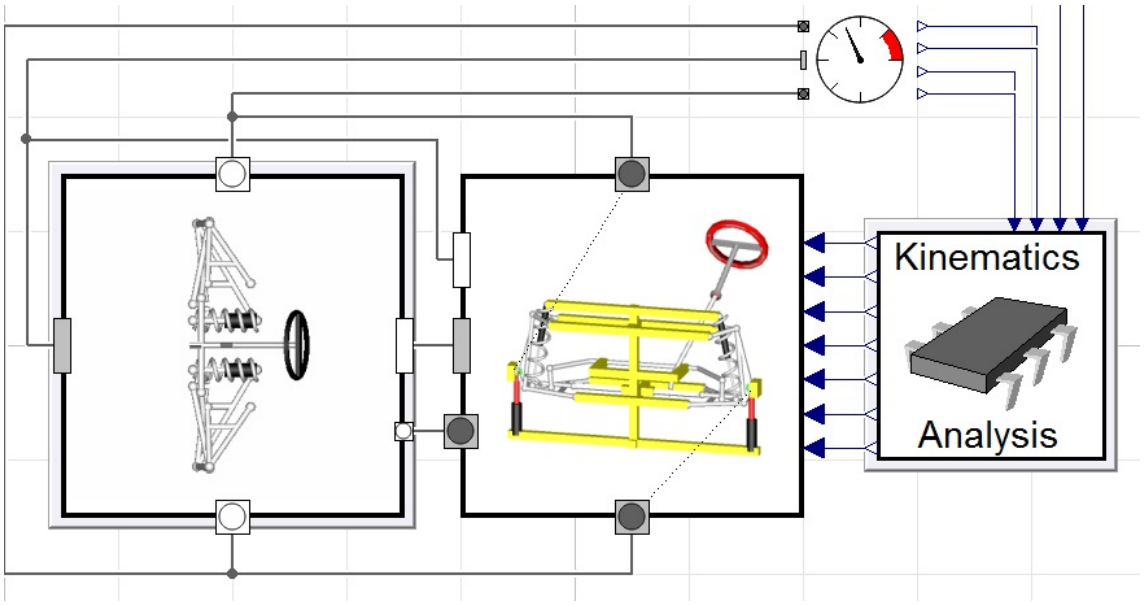

Figure 4.6: The K&C-rig in Dymola

On both axles heave and roll were simulated. As the car is designed for a wheel travel of 25 mm bounce and jounce, this was what was simulated. In roll, the system was simulated with an interval of 5 mm. See the first rows in table 4.1 to get an idea. To test the steering, the same kind of test was done, but this time with steering input with an interval of 20°, this is also illustrated in table 4.1.

To test the ARB, a somewhat different setup was needed due to the definition of ARB in Panthera, hub force per meter deflection. This was done by first setting the spring rate and damper rate to 0, that is, detach both of them. By placing one hub in it's design position with an actuator and then deflecting the other wheel as described earlier, the only forces acting on the actuator are the ones transferred by the ARB. The reaction force in the actuator could then be found in the parameter *rig.actuatedPiston_2.frame_a.f*.

4.5 Generating suspension parameters

The data generated by Dymola was not directly translatable to Panthera parameters and thus manual post processing was needed. The software chosen for this was Matlab. Panthera often uses linear values. However, the suspension parameters almost never behave exactly linearly in real life. Most of the time though, they behave linear enough to make a linear approximation of the behaviour, see figure 4.7 for an example. Where a linearization was deemed appropriate, the built in function polyfit in Matlab was used. A complete list of the suspension parameters generated for Panthera can be found in Appendix B together with an explanation of how it works in Panthera.

Table 4.1: Testing scheme for simulated K&C-test. First two columns represent the ΔZ hub position of each wheel. Third column represents the steering input.

Left wheel	Right wheel	Steer
-0.025	-0.025	$-90°$
-0.025	-0.020	$-90°$
⋮	⋮	⋮
-0.025	0.020	$-90°$
-0.025	0.025	$-90°$
-0.020	-0.025	$-90°$
⋮	⋮	⋮
0.025	0.025	$-90°$
-0.025	-0.025	$-70°$
-0.025	-0.020	$-70°$
⋮	⋮	⋮
0.025	0.025	90°

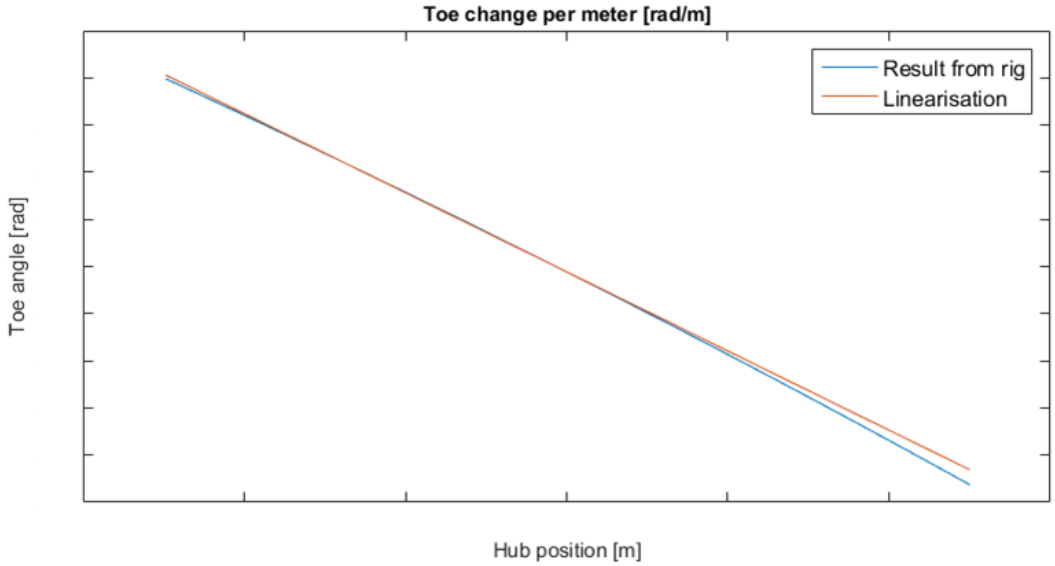

Figure 4.7: Toe angle induced by wheel travel on the rear axle

Anti-dive and **anti-squat** were both calculated in Matlab, according to section 3.3.3.

4.6 Roll center calculation

Roll-center was calculated by first finding the suspension pivot center in the y-z-plane. The pivot-point is found by drawing a line from the lower and upper upright positions to the lower and upper chassis attachment points. As the chassis attachment points did not have the same coordinates in the y-z-plane the midpoints were used to find the pivot-point, see figure 4.8.

The roll-center was then found by drawing a line from the contact patch to the pivot-point and finding the point where this line intersect the vehicle center line, see figure 4.8.

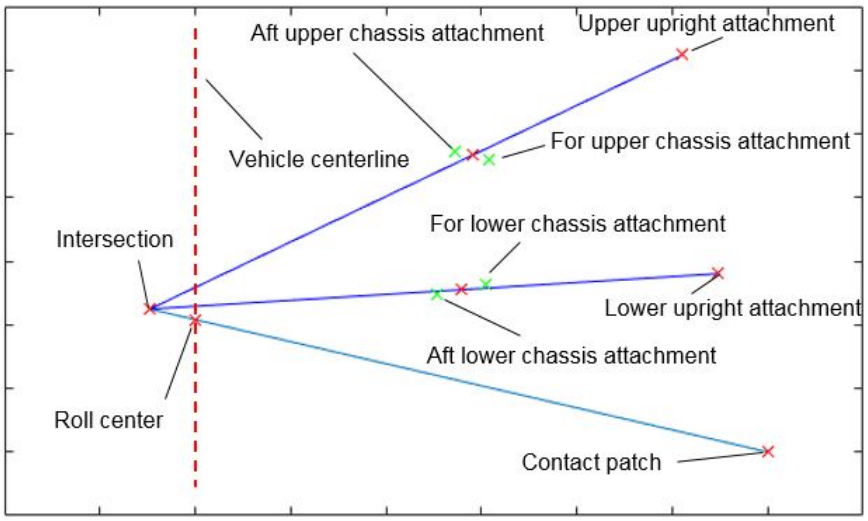

Figure 4.8: Upper and lower arm line intersection

4.7 Generating wheel orientation parameters

Caster offset was calculated by finding the intersection of steering axis and the ground and measuring the distance from the intersection to tire contact patch, see figure 4.9a. In Panthera, the caster angle is not implemented, instead it must be accounted for in the caster offset to get the correct length. This was done with equation defined in (4.4). Here $L_{caster,P}$ is the caster offset when compensated for Panthera. L_{caster} is the caster offset, otherwise known as mechanical trail.

$$L_{caster,P} = \cos\left(\alpha_{caster}\right) \cdot L_{caster} \tag{4.4}$$

Caster angle was calculated as the angle of the steering axis using the same hard points as by caster offset, see figure 4.9a.
Kingpin offset, or scrub radius, was calculated in a similar way to caster offset. As seen in figure 4.9b, it was calculated from the length from the intersection of steering axis and ground to the contact patch. Kingpin angle is not implemented in Panthera and thus the same method as for caster offset was used to compensate.

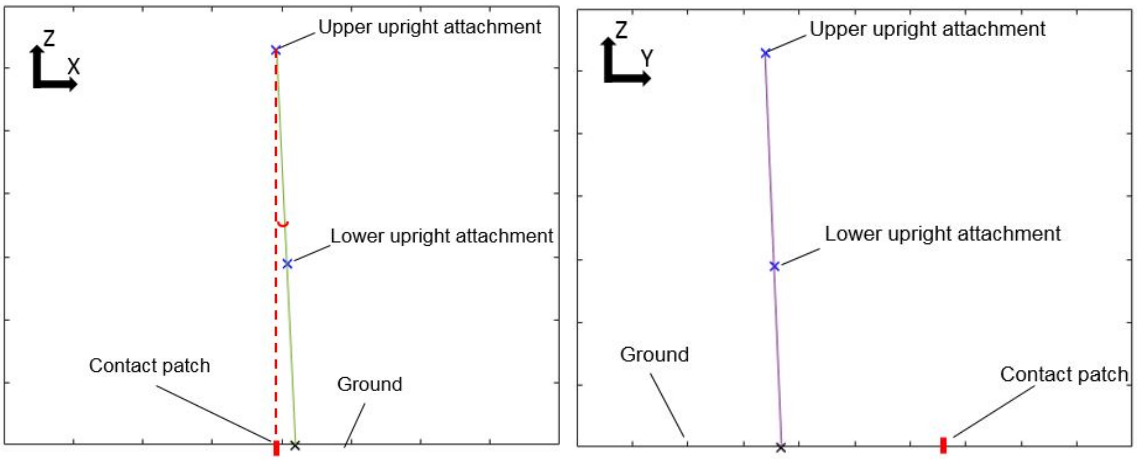

(a) Caster calculation **(b)** Kingpin offset calculation

Figure 4.9: Caster and Scrub radius calculations

Toe and **camber** needed some extra attention. As bump steer and bump camber are defined in Panthera as linear equations with origin at the free length of the spring, as opposed to the design position that would be the convention. This means that when the vehicle is put at rest, these effects will add onto the static values and can alter them quite much. To compensate for this, the equation in (4.5) was used. The following definitions apply:

- α_s refers to the camber or toe angle to be entered into Panthera
- α_d refers to the camber or toe angle desired at design position
- k refers to the geometry effect factor, for example bump steer
- L_f refers to the free length of the spring i Panthera
- L_d refers to the length of the spring when in design position

$$\alpha_s = \alpha_d + k \cdot (L_d - L_f) \tag{4.5}$$

4.8 Tire Modeling

The modeling of the Hoosier R25B tire used on the CFS17 car was made in the modeling software Optimum Tire. Raw tire test data produced by Calspan for the purpose of serving Formula Student teams and related projects was used for tire curve fitting. The tire curve fitting resulted in a Pacejka model which was later transferred to Panthera, and from which parameters could be determined. In order to establish the loads under which the tires are operating, a load case estimation was done. This was made with the use of logged data from FSGE.

4.8.1 Load Case Estimation

The load case estimation was done by quantifying the roll stiffness distribution and calculating the weight transfer on each axle accordingly. Logged measurements of acceleration, velocity and damper travel during the FSGE event was used for the calculations in this section. This ensured that the loads calculated were the ones

on the real vehicle. It meant that compliance in the system such as for example bushings was included [15]. However, it does not include the tire roll due to tire wall deflection. The parameters used for the equations in this section are described in table 4.2.

4.8.1.1 Roll Stiffness Distribution

The total roll angle of the car body was calculated according to equation (4.6), where x represents the suspension movement. The roll angle was likewise calculated separately for each axle in order to give possibility for roll stiffness distribution calculations, see equation (4.7).

$$\alpha_{roll} = \tan^{-1}\left(\frac{(x_{suspLF} - x_{suspRF}) \cdot MR_F + (x_{suspLR} - x_{suspRR}) \cdot MR_R}{TW}\right) \tag{4.6}$$

$$\alpha_{rollAXLE} = \tan^{-1}\left(\frac{(x_{suspLAXLE} - x_{suspRAXLE}) \cdot MR_{AXLE}}{T_{AXLE}}\right) \tag{4.7}$$

The degree of roll was plotted with the lateral acceleration for each set of data points. A linear curve fit was then made to match the data values. This is represented by the orange line in figures 4.10 - 4.12. The roll gradient could then easily be taken from this curve fit as it is defined according to equation (4.8) and thus to the slope of the fitted curve, meaning that the lower the roll gradient, the higher the resistance to roll movement. This was done for each axle as well as for the entire vehicle. This way of plotting the values is convenient since it directly shows the maximum roll angle and the lateral acceleration associated with it[15].

$$\text{Roll Gradient} = \frac{\text{degree of body roll}}{\text{lateral acceleration}} \tag{4.8}$$

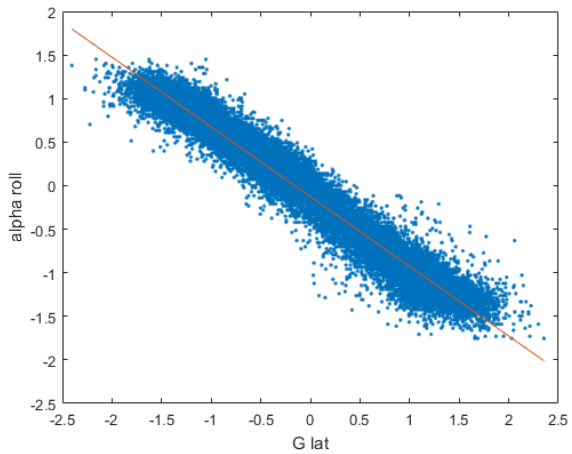

Figure 4.10: Roll of car plotted against lateral G force with corresponding curve fit

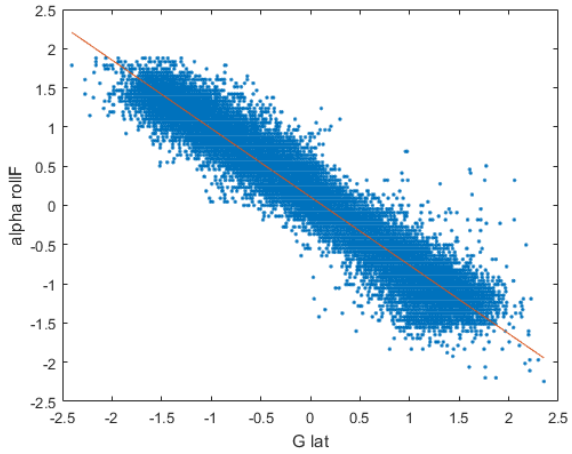

Figure 4.11: Roll of front axle plotted against lateral G force with corresponding curve fit

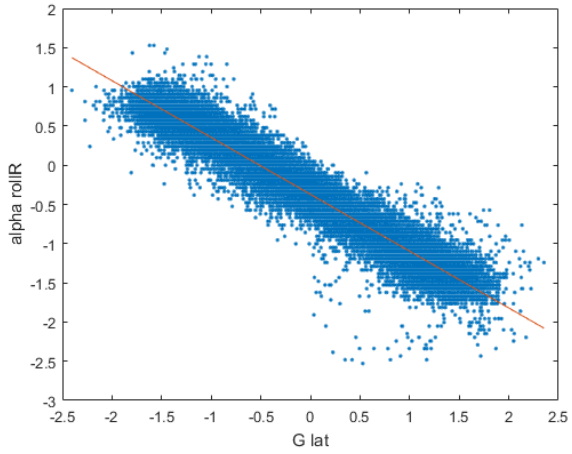

Figure 4.12: Roll of rear axle plotted against lateral G force with corresponding curve fit

The CoG height above roll axis was calculated according to equation (4.9) and the roll moment according to equation (4.10). The roll stiffness was then calculated for the total vehicle as well as for each axle, equation (4.11) - (4.13). The roll stiffness distribution was calculated with equation (4.14).

$$h_{roll} = h_{CoG} - h_{RCf} - \frac{(h_{RCr} - h_{RCf}) \cdot W_{sR}}{(W_{sF} + W_{sR})} \tag{4.9}$$

$$M_{roll} = h_{roll} \cdot (W_{sf} + W_{sR}) \tag{4.10}$$

$$K_{rolltot} = \frac{M_{roll}}{RG} \tag{4.11}$$

$$K_{rollf} = K_{rolltot} \cdot \frac{RG_r}{(RG_f + RG_r)} \tag{4.12}$$

$$K_{rollr} = K_{rolltot} - K_{rollf} \tag{4.13}$$

$$q = \frac{K_{rollf}}{K_{rollf} + K_{rollr}} \tag{4.14}$$

Table 4.2: List of parameters

α_{roll}	Roll angle of the whole car
α_{rollF}	Roll angle front
α_{rollR}	Roll angle rear
RG	Roll gradient
h_{roll}	Distance between CoG and roll axis
h_{CoG}	CoG height
h_{RCf}	Roll centre height front
h_{RCr}	Roll centre height rear
h_f	Front unsprung centre of gravity
W_{sF}	Sprung weight front
W_{sR}	Sprung weight rear
W_{sTot}	Total sprung weight
W_{uF}	Unsprung weight front
W_{uR}	Unsprung weight rear
ΔW_{sAXLE}	Sprung weight transfer
ΔW_{uAXLE}	Unsprung weight transfer
ΔW_{gAXLE}	Geometric weight transfer
M_{roll}	Roll Moment
$K_{rolltot}$	Total roll stiffness
K_{rollf}	Roll stiffness front
K_{rollr}	Roll stiffness rear
G_{lat}	Lateral acceleration
TW	Track width
WB	Wheel base
l_r	Distance from CoG to rear axle
l_f	Distance from CoG to front axle
MR_f	Motion ratio front
MR_r	Motion ratio rear
R	Wheel Radius

4.8.1.2 Weight Transfer

Calculations were made separately for weight transfer of the unsprung mass, sprung mass and the geometrical weight transfer. Since the FSGE track is located on a flat surface, banking was assumed to be zero. The unsprung mass includes the tires, wheels, brakes, and an appropriate portion of the suspension links and drive shafts, in this case approximately 50% [15]. The weight transfer due to unsprung mass was calculated according to equation (4.15) for each axle. Geometrical weight transfer

includes the forces coming from the tires and going through the roll center at the each axle. This was calculated according to equation (4.16). During cornering the sprung mass is essentially represented by the chassis of the car rolling, causing weight transfer. This weight transfer was calculated according to equation (4.17).

$$\Delta W_{uAXLE} = \frac{W_{uF} \cdot G_{lat} \cdot h_f}{TW} \tag{4.15}$$

$$\Delta W_{gAXLE} = \frac{W_{sF} \cdot G_{lat} \cdot \frac{l_r}{WB} \cdot h_{RCf}}{TW} \tag{4.16}$$

$$\Delta W_{sAXLE} = \frac{W_{sTot} \cdot G_{lat} \cdot h_{roll} \cdot q}{TW} \tag{4.17}$$

4.8.1.3 Downforce Estimation

The aerodynamics of the CFS17 car provides a substantial amount of downforce. A downforce estimation was done from the logged data, using the logged velocity. This is presented in figure 4.13, which is showing the downforce plotted against velocity. The very high downforce levels at speed proves that the downforce has to be accounted for in the load case estimation.

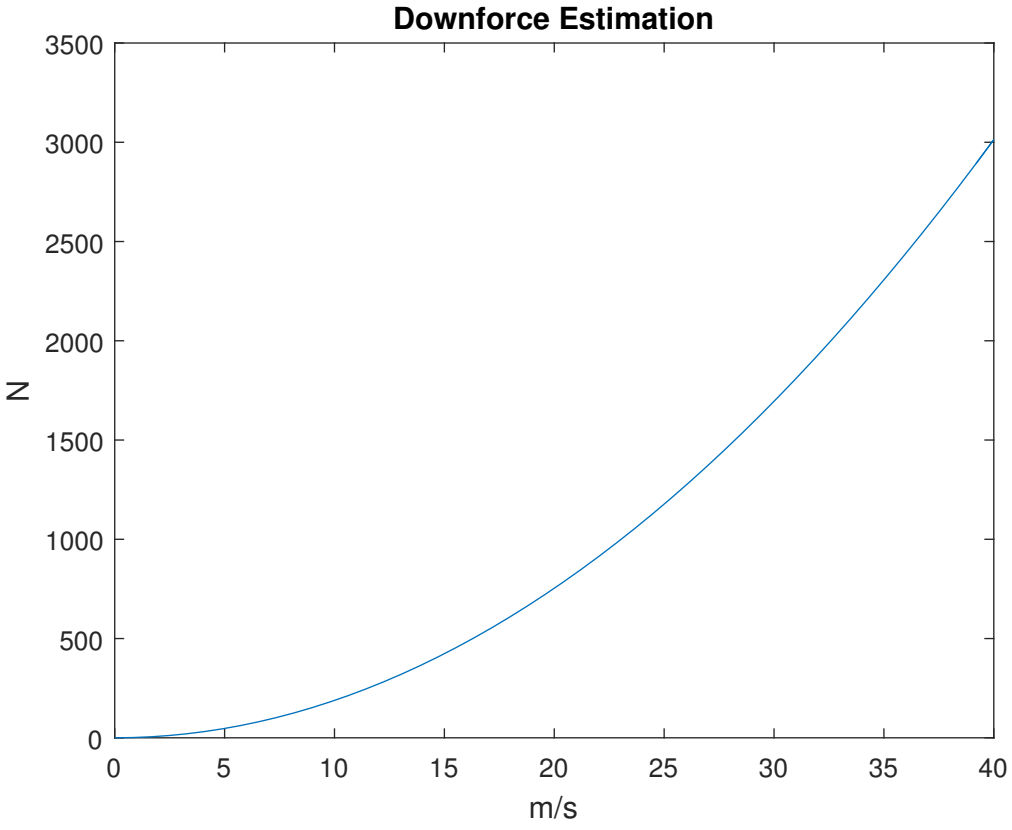

Figure 4.13: Downforce estimation

4.8.1.4 Braking

From the ax - ay plot shown in figure 4.14 it was observed that the vehicle is at most decelerating with 1.5 G, this though the car was designed to cope with 2 G. The braking torque needed to lock all four wheels was thus calculated for both cases. The longitudinal load transfer on the desired axle with static load N_{AXLE}, mass m and acceleration a was obtained by equation (4.18). The brake torque to lock both wheels on the desired axle was then calculated with equation (4.19). The computed brake torques can be found in table 4.3.

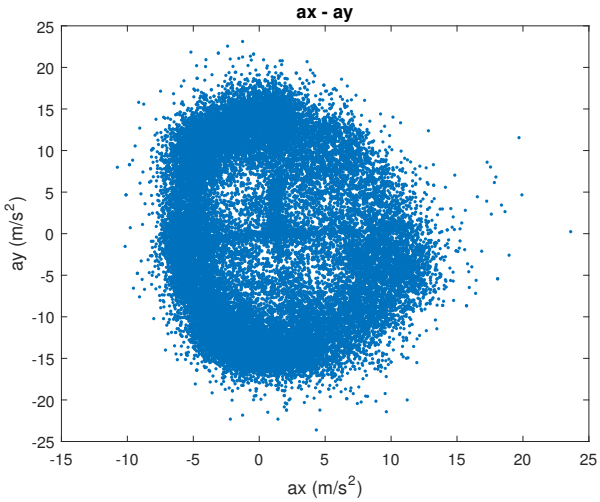

Figure 4.14: Longitudinal and lateral acceleration achieved at FSGE event(acceleration negative, deceleration positive)

$$F_{AXLE} = N_{AXLE} + \frac{m \cdot a \cdot h_{CoG}}{WB} \tag{4.18}$$

$$T_{AXLE} = \mu \cdot F_{AXLE} \cdot R \tag{4.19}$$

Table 4.3: Brake torque to lock all four wheels under deceleration

G	Front	Rear	Brake Bias
1.5	749 Nm	272 Nm	0.73 Front
2	840 Nm	170 Nm	0.83 Front

4.8.1.5 Final Load Case

From the load case estimation, figure 4.15 was established. From these the RMS and mean dominant high load values were taken. The tire was analyzed for the loads specified in table 4.4.

Table 4.4: Endurance Load Case

Static load	680 N
Mean RMS load	860 N
Mean dominant high load front	930 N
Mean dominant high load rear	1250 N

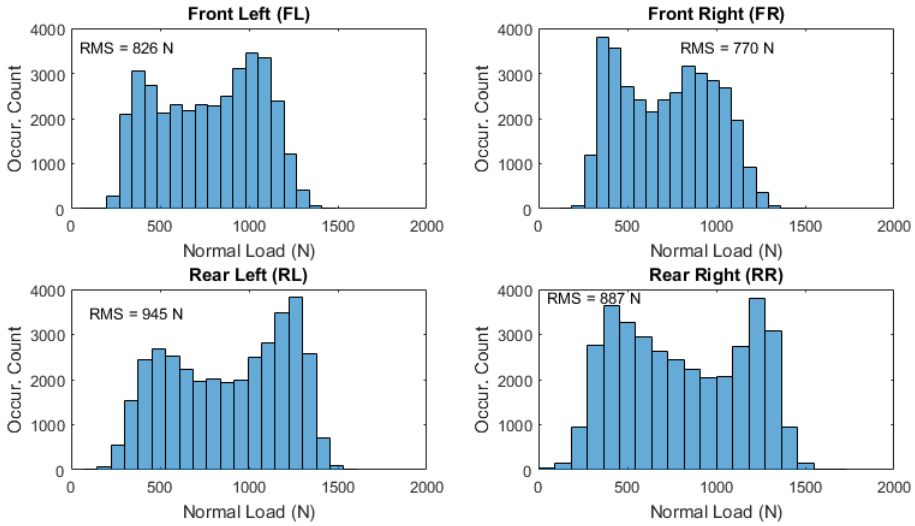

Figure 4.15: Histogram of normal loads and corresponding RMS values for FSGE

4.8.2 Model Fitting

Optimum Tire was used for the model fitting of the raw tire test data, which was made according to the procedures recommended in the documentation of the software. Two approaches of model fitting were made. The first included fitting a MF 5.2 model to the raw data, and then directly generating a tire file with the modeling software. The second strategy involved modeling a Pacejka 96 curve, which was then matched in the tire modeling tool provided by Cruden. Both strategies are further explained in this section.

4.8.2.1 MF 5.2 Modeling

The reason for the MF 5.2 curve fit was the possibility for Panthera to directly read and use a generated tire file without any manual interference. Raw tire data was fitted according to the fitting schedule specified, in table 4.5, making sure that the final error was as low as possible and not exceeding the acceptable boundaries

prescribed in the Optimum Tire tutorials[16]. The error was computed with the least squares method shown in equation (4.20). Error boundaries were not exceeded for the first 4 steps, while the last showed poor convergence and was therefore not used for the analysis of tire performance in this project.

Table 4.5: Model fitting order for pure lateral and combined data, Fit = Fit; Fe = Fit and calculate error

Model Fitting with Pure Lateral and Combined Data													
Step	Data Used	Coefficients to be Fixed						Coefficients to be Fit					
		Pure			Combined			Pure			Combined		
		Fx	Fy	Mz	Fx	Fy	Mz	Fx	Fy	Mz	Fx	Fy	Mz
1	Pure Lat.								Fe				
2	Pure Lat.		Fix							Fe			
5	Combined.		Fix	Fix				Fit			Fe		
4	Combined.	Fix	Fix	Fix	Fix							Fe	
5	Combined.	Fix	Fix	Fix	Fix	Fix							Fe

$$error = \frac{\sqrt{\sum (Model - Data)^2}}{\sum |Data|} \tag{4.20}$$

According to [10], the software should have the ability to read the generated tire file. While trying to accomplish this, a number of problems occurred, ranging from the reading of the file to unexpected vehicle behaviour in Panthera. Attempts were made to resolve these problems in collaboration with Cruden. Because of lack of time the approach was discarded and the second strategy was used instead.

4.8.2.2 Pacejka Modeling

Panthera offers a built in way of modeling tire curves, which uses Pacejka 89 [10]. Optimum Tire offers a range of different models, though not Pacejka 89. The Pacejka 96 model was considered closest to what was used in Panthera and was then used for the model fitting. As in the first case, the curve was fitted according to the fitting schedule in table 4.5 where the error was made sure to be under the error boundaries. As in the MF 5.2 curve fitting step 5 did not converge well and was therefore not used for tire analysis. Figure C.1 and C.2 shows the fitted Pacejka curves with corresponding raw data at the loads for which the tire was tested.

The tire curves were computed for the specified load cases in table 4.4 and are shown in figure C.3 - C.6. These were used as a baseline for the manual curve fit made in Panthera, which was made to the load case specified in table 4.6. The reason for the difference in tire load cases was the fact that the Panthera model fitting tool only allowed certain loads to be visualized.

Table 4.6: Panthera Modeling Loads

Static load	690 N
Mean RMS load	870 N
Dominant high load front	930 N
Dominant high load rear	1260 N

The manual curve fitting involved adjusting the a, b and c parameters seen in the Panthera curve fits, shown in figure C.7 - C.9. This was done by matching the peak longitudinal and lateral forces for the corresponding slip ratio and slip angle for the specified load cases in table 4.4. In the same way the peak aligning moment was matched with corresponding slip angle. The Panthera tire model was then further tuned during the driver sessions in order to get the correct subjective correspondence.

The optimal slip angle and slip ratio of the tire were directly generated in the Panthera model. The tire rate for the R25B compound was given on request by the tire manufacturer. This value was taken for 14 PSI which was the desired warm tire pressure used during FSGE. The rolling coefficient of the tire could not be generated through the modeling, meaning it had to be determined with other data. After consultation with the CFS team a rolling coefficient value was given, which was deemed to be reasonable [6]. The tire damping- and relaxation length related values were not given in the manufacturer specifications nor could they be obtained through the tire modeling. Because of this the standard values in Panthera was kept but slightly tuned during driving sessions.

4.9 Driving sessions

To evaluate the subjective assessment, a driver with experience from the real car was deemed to be necessary. A driver from last years competition was available for this assessment. The driver also had experience driving the simulator. The sessions were divided into multiple runs, where parameters were tuned after each run. A questionnaire, see appendix A, was answered by the driver to get input on how the vehicle behaviour changed when tuning different parameters. The driving was first carried out without motion to evaluate the basic car behaviour and was activated when the car was deemed to be performing well.

5

Results

5.1 Suspension

Generally the kinematic behaviour of the suspension in Panthera was very close to what was simulated in Dymola. The effects of **bump steer** and **bump camber** can be seen in figure 5.1 and 5.2 respectively. The results were similar for the rear suspension.

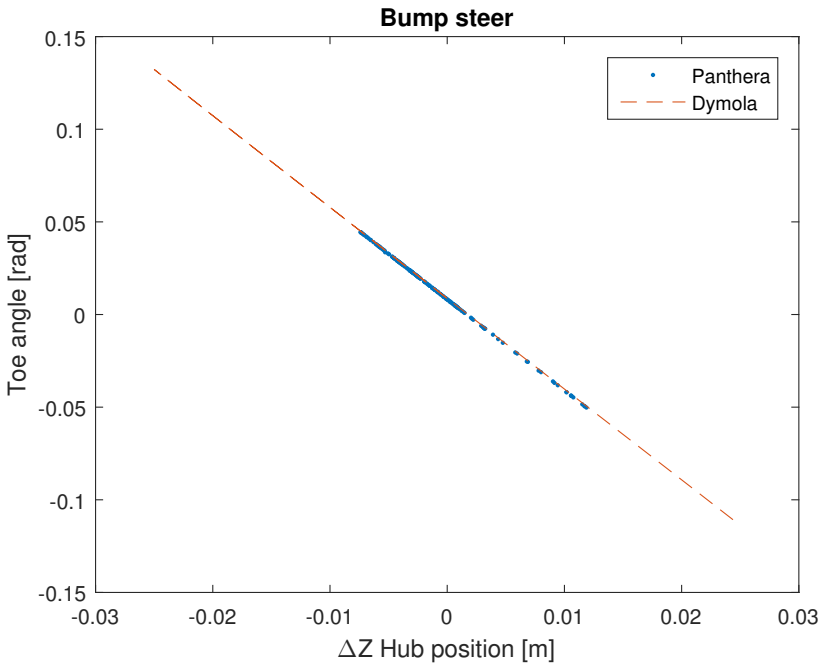

Figure 5.1: Toe angle induced by hub deflection

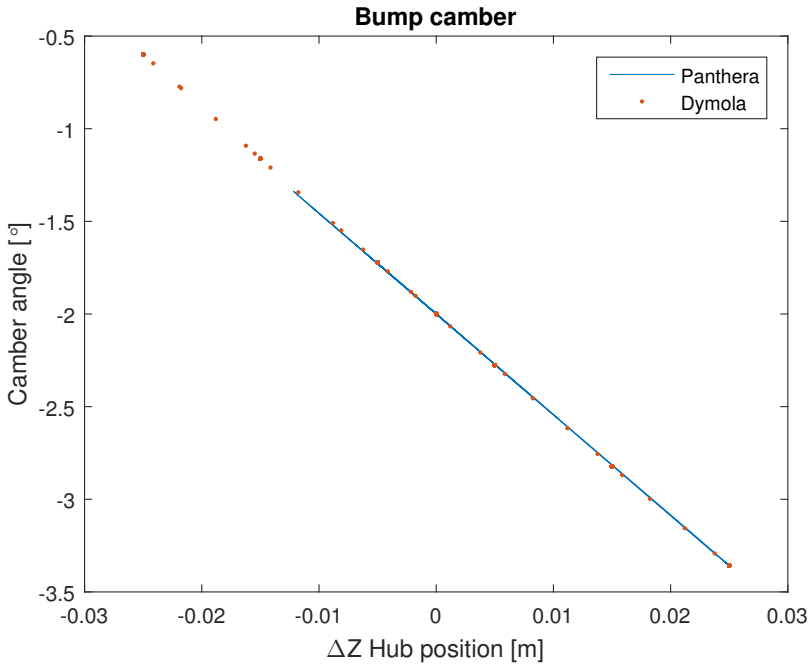

Figure 5.2: Camber angle induced by hub deflection

The actual **Ackermann** effect is not linear, as can be seen in the Dymola result, figure 5.3. The figure shows that the Ackermann effect in Panthera is quite similar to Dymola, especially for higher steering inputs. This is where the Ackermann effect makes a big difference. The two curves cross the origin on different sides and hence has different static toe. This is due to effects such as bump steer, since the tests could not be conducted at the same hub height.

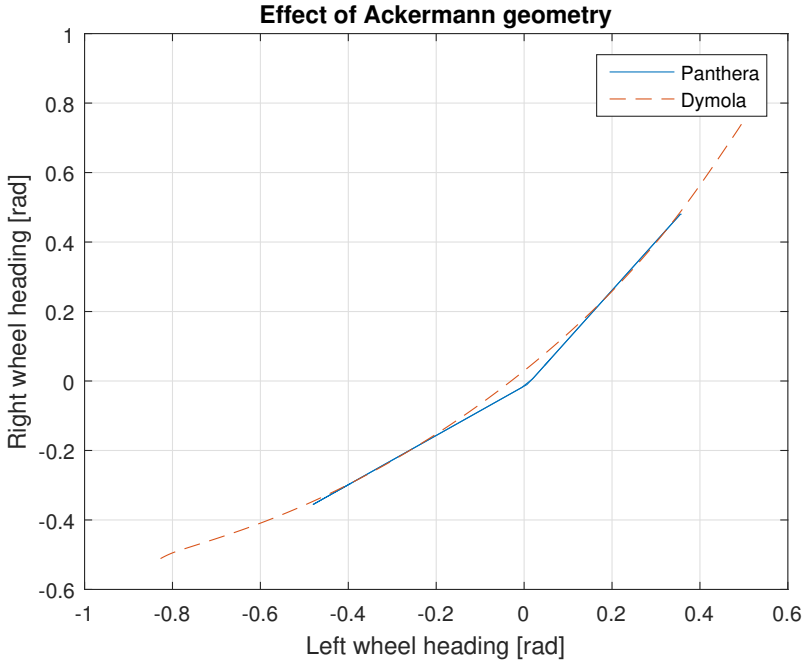

Figure 5.3: Difference in steer angle on front wheels due to Ackermann geometry

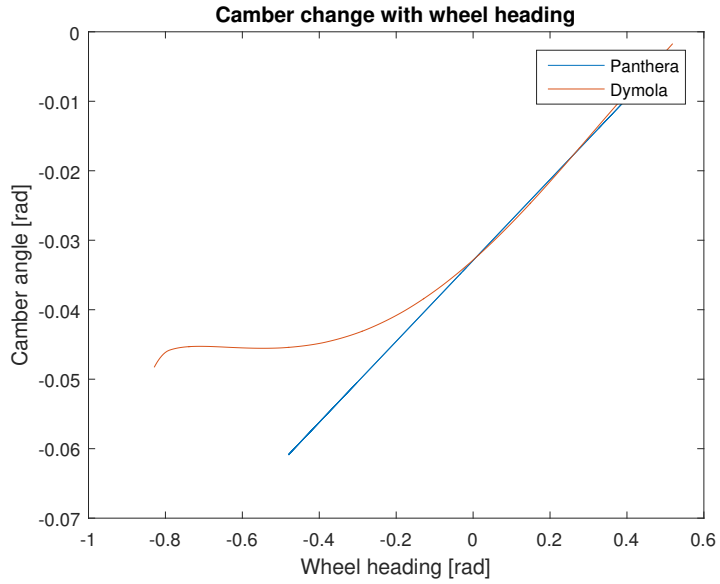

Figure 5.4: Camber angle induced by wheel steer angle on left front wheel

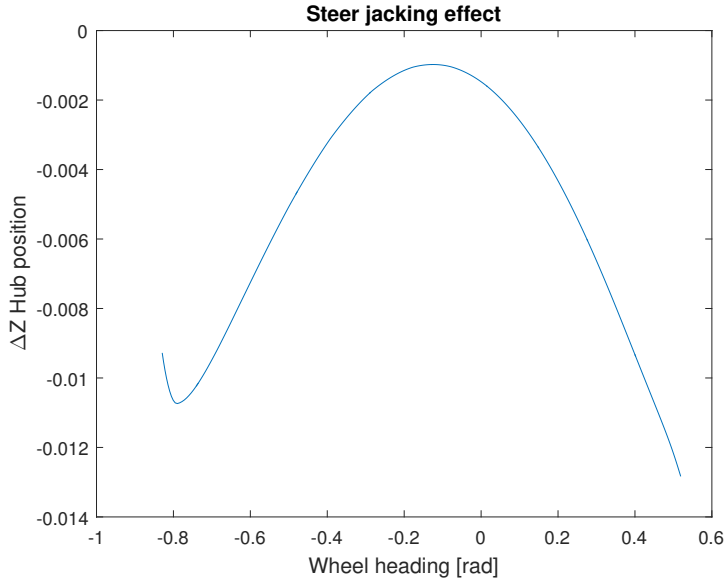

Figure 5.5: Jacking effect induced by steer angle in Dymola

Due to the design of the suspension geometry, the **camber induced by steering** was not linear during steering with negative toe angle. Hence a linearization was based on steering input in the other direction. Figure 5.4 shows that Panthera followed the simulation results from Dymola very close in that region.

The effect of **steer jacking** was not linear. This is illustrated in figure 5.5. Due to this quadratic shaped curve having a center approximately around 0, no linearization could be justified. Hence the decision was taken to not implement the steer jacking effect in Panthera.

Looking at the ARB, the results from Dymola gave a relatively low stiffness. As the ARB can be adjusted in the CFS car, this was considered a good starting point. This value was later tuned during the simulator runs. The value that was used was obtained from figure 5.6, where it can be seen that the linearization co-relates well with the Dymola results. When looking at data from the simulator runs, figure 5.7, the roll stiffness indeed seemed low compared to the results from section 4.8.1.1.

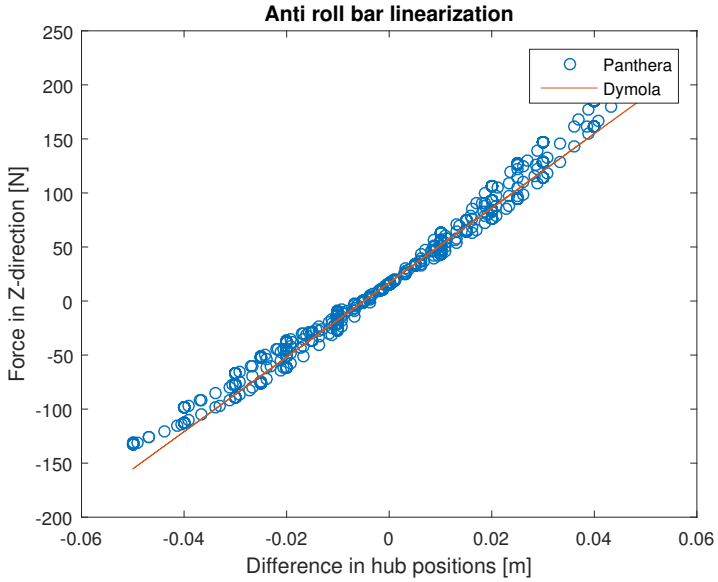

Figure 5.6: Scatter plot of force distribution resulting from the ARB together with the linearization of the same

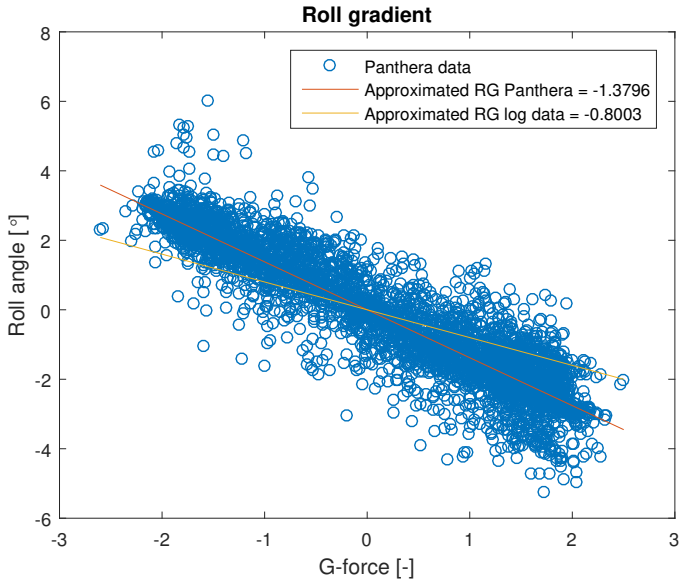

Figure 5.7: Scatter plot of roll angles of vehicle at different lateral accelerations with approximated linearization

5.2 Tire Modeling

The tire model generated in Optimum Tire was validated by analyzing the correspondence with the raw tire test data and further studied by considering the specific load case. The Panthera tire model was then compared with the model obtained from Optimum tire. These evaluations are discussed below.

5.2.1 Optimum Tire Results

When analyzing the Optimum Tire model in figure C.1 and C.2 it is clear that it highly corresponds to the raw tire test data for the tire testing loads. Further analyzing the Optimum Tire model at the calculated load cases in table 4.4, the model shows reasonable curves in figure C.1 and C.6. The curve representing longitudinal force versus slip ratio, shown in figure C.3, is experiencing an arguable behaviour where it is only crossing the origin at static load, and shifts horizontally with increased load. This is believed to be caused by the way the tire has been tested but was not further investigated due to time constrains.

5.2.2 Panthera Tire model Results

Table 5.1 shows the peak values at the specified load cases for the Optimum Tire model and Panthera model. Looking at the Fy peak values, it is observed that the friction coefficient decreased with increased load for both models. In contrast the optimal slip angle for the Optimum Tire model is increasing with added load, while for the Panthera model it is decreasing. One can also see that both the friction coefficients and optimal slip angles are close at static load, though somewhat bigger for the Optimum Tire model. Further looking at the Fx peak values the models are close to identical at static load and with increased normal force the optimal slip ratio for both models are closely corresponding. The friction coefficients at static load are very closely matched, but when increasing the load, the Optimum Tire model increases its friction coefficient while it is decreasing for the Panthera model. The aligning moment values are very closely corresponding and are following the same general trend. The Optimum Tire model has faster increase in both friction coefficient and optimal slip angle for increased load. The Optimum Tire model is in relation to the Panthera model thus reaching bigger peak values for higher loads, and simultaneously lower values at loads close to static.

Table 5.1: Peak values at specified load cases for Optimal Tire model and Panthera model

Optimum Tire			Panthera		
Fy Peak			Fy Peak		
Load (N)	mu	SA (deg)	Load (N)	mu	SA (deg)
680.0	2.57	11.0	690.0	2.33	10.07
860.0	2.5	12.0	870.0	2.20	9.79
930.0	2.41	13.0	930.0	2.15	9.66
1250.0	2.36	14.5	1260.0	1.90	8.97
Fx Peak			Fx Peak		
Load (N)	mu	SA(deg)	Load (N)	mu	SR
680.0	2.28	0.16	690.0	2.28	0.12
860.0	2.32	0.12	870.0	2.15	0.11
930.0	2.36	0.11	930.0	2.10	0.11
1250.0	2.4	0.095	1260.0	1.85	0.10
Mz Peak			Mz Peak		
Load (N)	Nm	SA (deg)	Load (N)	Nm	SA (deg)
680.0	34.0	3.0	690.0	35.09	4.0
860.0	44.0	3.5	870.0	43.31	4.14
930.0	49.0	3.6	930.0	45.95	4.28
1250.0	78.0	5.0	1260.0	59.77	4.55

5.3 Validation

The vehicle model was validated with objective metrics by comparing logged data from CFS to what was gathered in the simulator runs. This was roughly done by comparing load cases, accelerations and velocities. The influence of not implementing a torque vectoring system was also investigated. This was done based on both objective metrics and subjective assessments.

5.3.1 Load Case Correlation

Loads achieved on each wheel during simulator driving are shown together with corresponding RMS values in figure 5.8. The resulting load case is shown in table 5.2. Comparing the load case from the simulated driving and FSGE event, both the mean RMS value and the dominant high loads front and rear are higher in the simulated runs. One reason for this is believed to be the fact that the simulated car is modeled with a 80 kg driver while the logged data was gathered from a run with a 70 kg driver. During the simulator runs it was also observed that the car sometimes was experiencing unrealistic behaviours where it bounced when hitting

some of the bumps on the track. This may have had an effect on the load case since the wheels during these occurrences sometimes left the ground causing a higher load at impact. It is unknown how the tire model itself experienced these forces, though no undesired forces were observed.

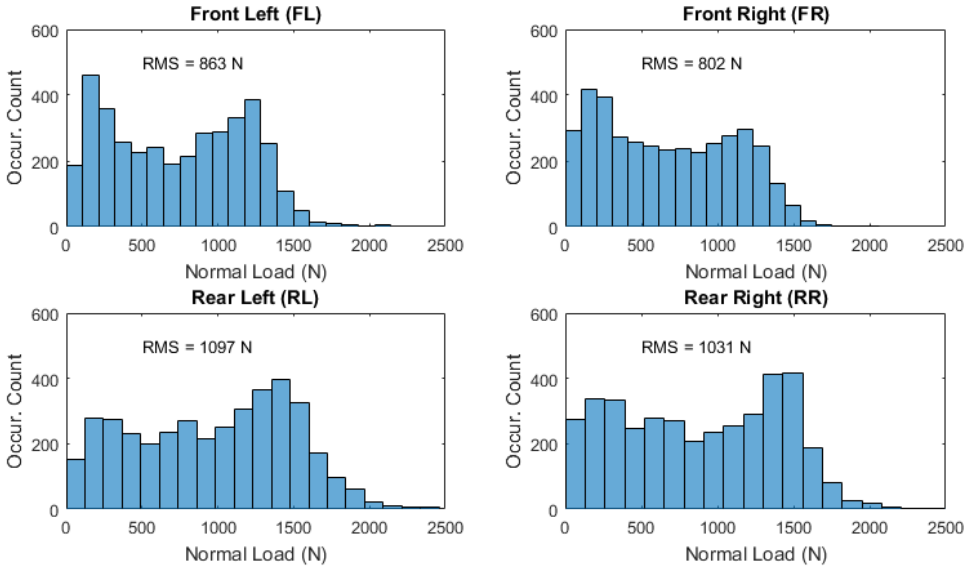

Figure 5.8: Time histogram of normal loads and corresponding RMS values on each wheel from simulator runs

Table 5.2: Simulator Load Case

Static load	680 N
Mean RMS load	948 N
Mean dominant high load front	1154 N
Mean dominant high load rear	1401 N

5.3.2 Acceleration

The accelerations obtained in Panthera can be seen in figure 5.9. Comparing to accelerations reached in the logged FSGE run seen in figure 4.14 it becomes clear that the simulator run closely corresponds to the FSGE run. During hard braking the vehicle reaches 1.5 G and during acceleration 1 G. When looking at the lateral acceleration the same close correlation is observed. Here both runs are reaching 2 G. Figure 5.10 shows the lateral and longitudinal accelerations separately for both runs. It is observed that the accelerations are broadly correlating and that similar approximate magnitudes are reached in the same areas for both runs. Further analyzing the graphs shows that accelerations of approximately the same value are occurring at same parts of the track, though the simulator run overall is showing slightly higher values.

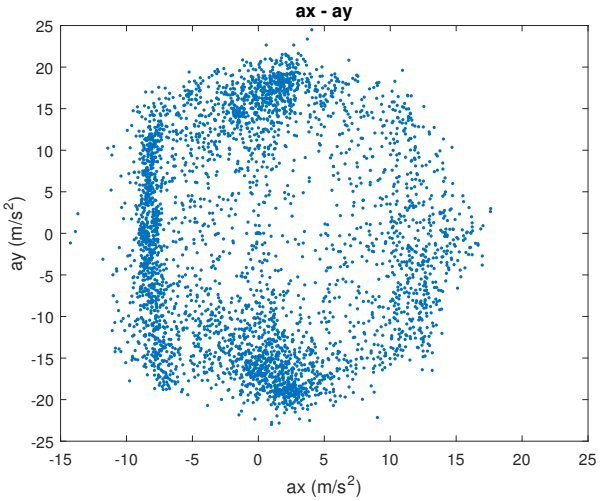

Figure 5.9: Longitudinal and Lateral acceleration achieved in simulator driving

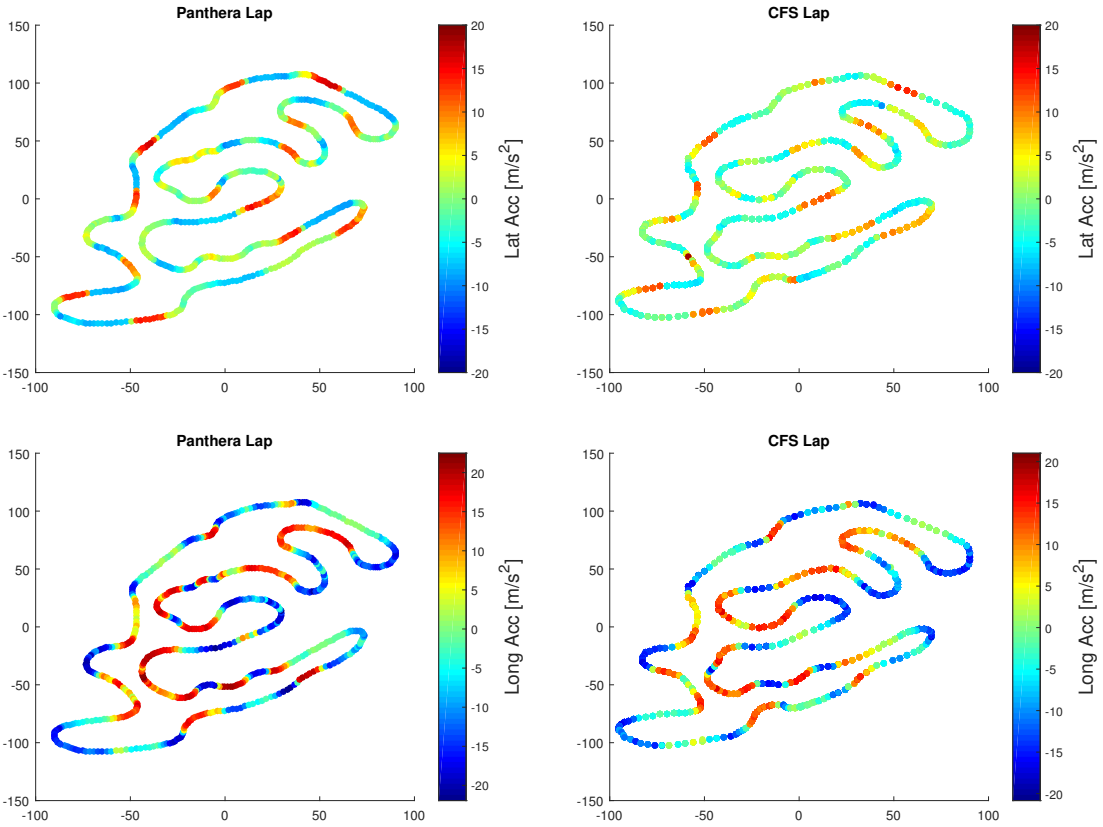

Figure 5.10: Longitudinal and lateral acceleration acceleration plotted from real driving and simulator driving

5.3.3 Velocity

As with the acceleration the velocity of the vehicle during the logged FSGE run and Panthera driving was compared. The simulator run closely follows the velocity

trends of the real vehicle, though generally showing somewhat higher values at long straights and lower values around the tighter corners. One reason for this is that the track itself does not exactly correspond to the real one.

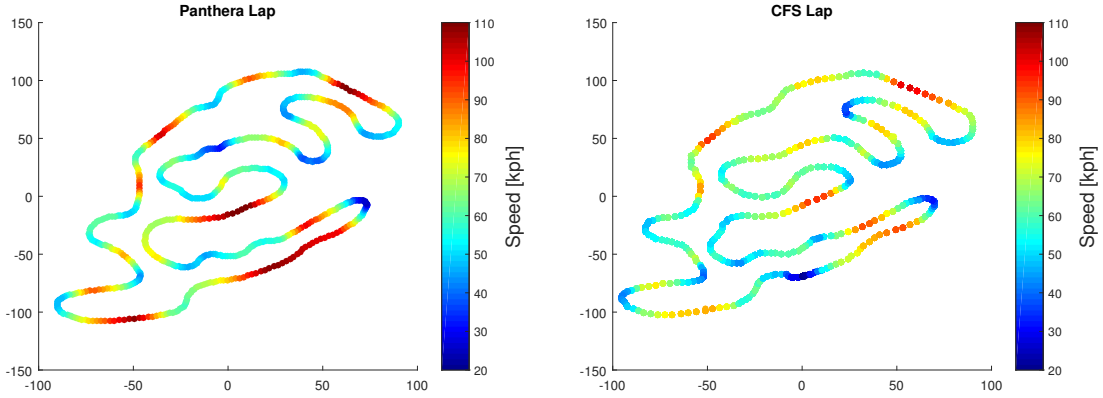

Figure 5.11: Velocity comparison for logged FSGE run and Panthera driving

5.3.4 Combined tire properties

The vehicle was modeled in Panthera without any torque vectoring system, instead using a limited slip differential. The comparison of yaw rates and yaw accelerations showed similar values, though the yaw acceleration was slightly higher for the FSGE run. This comparison was not considered enough since two different systems under diverse conditions were compared. It was expressed by the driver during the simulator runs that he sometimes was missing the feel of the torque vectoring. This mostly during corner exit, where a lack of the rear end "kicking out" during acceleration was expressed. In order to analyze this, equation (5.1) was used to estimate the weighted potential usage of the rear axle.

Tires will under different normal loads generate different lateral forces. This is easily observed in the generated tire curves. By dividing the absolute applied force on the tire with the highest potential obtainable force under the given normal load, an indication of the potential use of that particular tire is given. The result of this is the percentage of how much of the potential force that is actually being used on that tire. This value is then squared and multiplied with the fraction of the potential of the considered wheel and the sum of the potential of both wheels on that axle. The second term gives a percentage of potential used on the considered wheel relatively to the potential of both wheels on the axle. This calculation is done for both wheels and then summarized. What is then obtained is what can be called the weighted potential usage of the considered axle. This calculation is represented by equation (5.1).

$$WPUA = \sum \left(\left(\frac{\sqrt{Fx_i^2 + Fy_i^2}}{Fpot_i} \right)^2 \cdot \frac{Fpot_i}{Fpot_{tot}} \right) \tag{5.1}$$

In order to obtain equation (5.1) an estimation of the forces acting on the wheel was needed. The normal loads were calculated according to the load case estimation described in section 4.8.1, whereas the longitudinal force was roughly estimated by equation (5.2), where the tire radius is multiplied with the torque. The lateral force was calculated through equations (5.3) - (5.5). Here the total generated lateral force is, as seen in equation (5.3), naturally taken up by the wheels at both axles. The proportion of this lateral force generated by the rear axle is derived through equation (5.4). Then an approximation of the lateral force generated by each of the wheels on that particular axle was done. Keeping in mind that the effect of slip angles was not considered it was assumed to be proportional to the normal force acting on that tire. This can be seen in equation (5.5). Here the N_i represents the normal load on the considered wheel and N_{tot} the summarized normal load of both wheels. The maximum potential of a tire is calculated according to equation (5.6). The summarized potential of both wheels is given by $Fpot_{tot}$.

$$Fx = R \cdot T_{wheel} \tag{5.2}$$

$$m \cdot ay = Fy_f + Fy_r \tag{5.3}$$

$$Fy_r = m \cdot ay \cdot \frac{l_f}{WB} \tag{5.4}$$

$$Fy_i = Fy_r \cdot \frac{N_i}{N_{tot}} \tag{5.5}$$

$$Fpot_i = \mu \cdot N_i \tag{5.6}$$

Once again considering the expressed lack of the rear "kicking out" during corner exits in the simulator run. It is known that by the way the torque vectoring system in the CFS17 car is designed, something that will not be explained in this report due to confidentiality, there is a point when accelerating out of a corner where the system may start giving equal torque to both wheels. Knowing that the normal and lateral loads on the tire cannot be directly controlled by the system, the only thing affecting how much of the tire potential that is being used is the longitudinal force. With this in mind there may be occasions during cornering exits where the system starts giving equal torque to both wheels causing one or both of the wheels to start using more of its potential. The tire may then saturate and the vehicle will start sliding. This can be the reason for the non existent feel of the rear kicking out during the simulator run. The limited slip differential in the modeled vehicle can be thought of as distributing the torque to the wheels passively and will then not give sudden equal torque distributions, thus obtaining smaller weighted potential usage of the axle during those specific occasions.

The calculations for the WPUA were made for both cases. Trying to find the point at which the earlier expressed phenomena occurred was discovered to be quite difficult and could thus not be properly investigated. Instead the calculations where done from mid corner to corner exit, which revealed that the WPUA for the CFS17 car was around 70% while for Panthera it was reaching 80%.

5.4 Driving sessions

In total 15 hours of simulator driving, split in three sessions, was done. During these sessions, the vehicle model was tuned as well as validated against subjective assessments. The overall comments from the driver at first was a lack of front grip. The high speed stability was also a problem, with extensive rolling in the corners. During the sessions, a large amount of time was dedicated to tire model tuning. The ARB was also tuned in order to reduce roll. There were some experiments made with adjustments of maximum braking torque, engine torque and anti-pitch values. At the end of the last session, the driver was pleased with the vehicle, describing it as well balanced and comparable to the real car. There were some problems other than the car during the simulator runs. At some parts of the Panthera track, the irregularities were larger than on the real track. Also the visual representation was commented upon. Here it was expressed that the lack of markings in the asphalt made it hard to drive consistently.

6
Discussion

6.1 General

The driver was not pleased with parameters sourced directly from the data at hand. There could be multiple reasons for this, ranging from calculations based on poor assumptions to data not being fully consistent with the car. Further work needs to be done if the simulator is to be a valuable source for CFS to use in an early design phase to examine different vehicle concepts. On the other hand, it has been shown that by tuning the model, a well made representation of the vehicle can be achieved, which is valuable when considering drivers practice.

6.2 Suspension Parameterization

The suspension modeling was in many ways successful. Many of the parameters calculated in Dymola were implemented into Panthera with good results. The biggest limitation in Panthera in this respect is the usage of linear models in many applications. For a racing car with few bushings and a small working range, this was not a big issue. The problems may grow with bigger and more general vehicles, where compliance in bushings and non-linear behaviour in the suspension occurs. Still, there is some compliance in all parts of a car, flexing chassis and flexing control arms to name some. Every bit of compliance that is not modelled will add to the error level. Some parameters in Panthera, such as dampers and springs, are able to use look up tables instead of linear equations. Some other parameters, such as steering related parameters, are able to use quadratic as well as linear equations. For most parameters though, this possibility does not exist. This meant that some types of behaviour, such as steer jacking, could not be modeled.

Other obstacles were the fact that Panthera in some parts does not follow conventions in vehicle dynamics. One such case is the definition of rest. By convention, a vehicle in rest refers to the design position, while in Panthera rest is defined as when the springs are at their free length. Panthera does use convention when for example defining the origin of the bump steer. It is defined as the amount of camber angle per deviation from rest position. With different definitions of rest position difficulties occurred during implementation.

6.3 Tire Modeling

The generated tire model made in Optimum Tire highly corresponded with the raw tire test data for lateral force and aligning moment. On the other hand the curve for the longitudinal force with slip ratio showed an arguable behaviour where it shifted horizontally with added load. For the higher loads it was also seen that the force dropped of more rapidly with increased normal force. A drop of after the peak value has been reached is natural for the tire, though the aggressiveness in the strongly increased drop can be questioned. This behaviour is, as earlier mentioned, believed to be a result of the way the tire is tested, but should be further investigated for clarification.

When manually modeling the tire in Panthera, it was initially done by matching the peak values in the model to the ones from Optimum Tire. This also gave opportunity to filter out the unwanted behaviour of the curve representing longitudinal force versus slip ratio, where it was observed to shift horizontally with increased load. When modeled, the tires were tested in Panthera, where additional tuning was made. This in order to get a representative feeling that corresponds with the real vehicle. Tuning was also made in order to mimic the overall behaviour of the car, which further affected the final curve fit. The changes made in the model were foremost done for the longitudinal and lateral forces, explaining the change in peak value trends seen in table 5.1. It can be argued whether the tire curves should have been tuned or not. The reason for the tuning of the curves was the fact that they were not used for comparison of different tires, but as a tool to mimic the environment the driver would have been operating under when driving the real vehicle. As earlier stated, the track used in Panthera may not have exactly corresponded to the actual FSGE track. With this in mind the modification of the tire model was considered to be somewhat justified.

Mentioned in section 4.8.2, is that the parameters related to tire damping and tire relaxation could not be obtained from the tire modeling. Likewise it could not be found through other sources. The chosen strategy was to use the default Panthera values and to tune them during simulator runs. These parameters may strongly affect tire performance and responsiveness, but was to some degree compensated for with the tuning of the model.

6.4 Aerodynamics

The aerodynamics in Panthera is quite simplified. It assumes longitudinal flow and a constant force coefficient. Panthera always use the car velocity as the fluid velocity, which implies conditions with no wind at all. In real life, this is far from true. In testing, the force coefficient is found to vary with the velocity. The assumption of longitudinal flow does not apply during windy conditions, where it is very often some kind of cross wind occurring. Also, if a wind is traveling directly in the longitudinal direction, it would alter the fluid velocity over the car. This reasoning also affects the downforce estimation done in section 4.8.1.3.

6.5 Engine and Driveline

The implemented torque curve is a well made representation of the one in the CFS17 car. What can be questioned is the fact that it is static, while the real torque curve somewhat changes with, among other things, temperature. This may cause some differences in the torque delivery relative to the CFS17 car. In the purpose of drivers training though, it can be argued that a static curve is more beneficial since it contributes to consistency.

Further considering the driveline being modeled as a LSD instead of an active TV-system some differences were found. For example the yaw acceleration was higher for the CFS17 car, which also showed a smaller WPUA value. These are significant differences and can be traced back to a lack of sufficiency in the way the torque is distributed in the Panthera model. Simultaneously there are many other factors affecting the behaviour of the car. The modeled tire is known to have different properties relatively to the Hoosier R25B used by CFS, which in this case becomes crucial, for example when considering WPUA. The tire pressure and temperature is assumed to be constant in the model whereas in reality it is in fact constantly changing. The friction coefficient is approximated based on the FSG track but not known and may also vary in reality. The differences when comparing the vehicle model and the real car is in some extent due to the non existent TV-system, but is also a result of other contributing factors.

6.6 Logged data

The load cases obtained from the FSGE run and simulator runs were closely corresponding with the simulator load cases showing slightly higher values for both mean RMS- and mean dominant high loads. This may, as mentioned in section 5.3.1, be due to the fact that the Panthera model was implemented with a 80 kg driver whereas the compared FSGE run was made with a 70 kg driver. Another reason for various loads is the difference in the driving environment. For example the vehicle in Panthera was sometimes experiencing bouncing behaviour on some parts of the track, causing higher loads on impact. Something worth considering is that the driver may also change driving style when driving the simulator to cope with

different driving conditions, which may affect the load cases. This was also observed during simulator runs, where the driving style was seen to sometimes change due to different vehicle settings.

Considering the acceleration and velocity, the Panthera run showed slightly higher values. As mentioned the track was in some cases not correctly representative of the FSGE track. The reason for this is believed to be that the track used for the Panthera runs is based and modeled upon GPS coordinates, causing some differences relatively to the real track. This means that some corners may not have been accurately picked up by the GPS and thus not correctly modeled. One such area is for example the long straight in the lower right corner of figure 5.11, where the Panthera graph is showing substantially higher velocity values than in the corresponding area on the logged FSGE lap. To be mentioned is also that the cones(track boundaries) were only visually modeled, meaning that the driver could drive through these without any interference. Keeping this in mind and considering the earlier mentioned observations of the driver sometimes slightly changing driving style, some variations in logged data was to be expected.

6.7 Driving sessions

The validation and tuning by subjective assessments was a success in that the driver was pleased with the behavior of the model in a comparable way to the real car. Controversially in order to reach this point, some parameters had to be altered and therefore not sourced directly from the real vehicle. Other valuable things that came from the subjective assessments was the importance of motion cuing and visual cuing. One thing that the driver pointed out was how the brake points were hard to find as there where no rubber marks on the track.

6.8 Conclusion

The work that has been done, resulted in a method going from vehicle data to a parameterized vehicle model for Panthera. The work also resulted in a model of the CFS17 car which will be valuable for future drivers training. Since a version of the Panthera software is available for free online, this thesis could also be used as a guide on how to implement vehicles in desktop simulators as well as widening the interest in vehicle dynamics.

6.9 Future work

The project has resulted in a well made implementation of the CFS17 car. However, there are multiple points that could be improved to further improve the fidelity of the model.

6.9.1 Steering feel

The steering torque as it is now, is not tuned at all. A scaling factor of 0.5 was preset, which together with the resulting aligning moment from the front wheels proved to be a reasonable. It should however be possible to calculate a correct value. Considering the fact that the steering wheel used in the simulator has a different radius than the one in the CFS17 car, it could be more appropriate to work with the tangential force of the steering wheel. The steering system acts as a lever for the wheel torque to the steering wheel. This could be carried out by calculating what the actual value is on the CFS17 car, then trying to find out what the lever is in the simulator. With this data known, one can adjust the force feedback factor to create equal torques or tangential forces.

6.9.2 Anti Roll Bar

The anti roll bar calculations in this work were basic, only accounting torsion of the bar itself. One should however also consider bending of the bar, as well as torsion and bending of the lever of the bar. This is explained very good with formulas in [17].

6.9.3 Torque Vectoring

The influence of modeling the vehicle with a LSD instead of a TV-system should be further investigated since the behaviour of the car may be possible to mimic through the tuning of other parameters. This was among other things aimed for during the work of this thesis. The difference in vehicle behaviour should also be investigated in more depth. This as it may be due to the differences in torque distribution, but also due to Panthera and simulator related properties. The implementation of a TV-system could be done through the scripting level in Panthera with active differentials. Matlab should be able to connect via UDP to the Onyx language which can be used to simulate an active differential in Panthera[10].

6.9.4 Tires

Further tuning of the tire models is recommended. What should also be explored is the use of various tire models, as well as the possibility of directly importing a tire file to Panthera. This would not only be more time sufficient, but would also reduce the error level as opposed to modeling the tires by hand.

6.9.5 Compliance

No compliance was considered in the kinematic calculations. In reality there is compliance in all parts of a vehicle. If compliance would be neglected in a part, which in reality is very flexible, the error would be extensive. For future work, identification of the source of large compliance could be done, with implementation in Panthera.

6.9.6 Track

Although the track has the correct layout, it is still somewhat different from the real counterpart. Further work could be done in order to enhance the correct feeling for the driver.

6.9.7 Human perception

A big feedback to the driver is the motion cue filter. As the simulator has limitations in its movements, it cannot recreate all the forces acting on a car. The motion cue defines how the simulator should translate these forces. During the driving sessions, the acceleration factor of the simulator platform had to be reduced due to the driver complaining about it feeling "too much like a roller coaster". This is an example of a motion cue that is not adapted to the particular use. The motion cue could be adjusted to fit the driver, car and track. This would enhance the experience for the driver a lot and thus recreating a more realistic environment. Other ways to enhance the experience would be devices like active belts, to simulate braking forces when a driver is pushed against the seat belt [18]. The collaboration with medicine could be valuable in order to elaborate how the human senses can be further used to evaluate vehicles in a DIL-simulator.

Bibliography

[1] Frisk, D. (2016) A Chalmers University of Technology Master's thesis template for LaTeX. Unpublished.

[2] Cruden, Panthera Software [Internet]. Amsterdam: Cruden; 2018 [cited date 2018-05-12]. Available from: http://www.cruden.com/panthera-software/

[3] Nationalencyklopedin [Internet]. Malmö: Nationalencyklopedin. L. Råde; 1987 - . [cited 2018-05-04]. Available from: http://www.ne.se/uppslagsverk/encyklopedi/lång/simulering

[4] Nationalencyklopedin [Internet]. Malmö: Nationalencyklopedin, Gunnar Grandin Hans Ulfhielm Lennart Strandberg Tore Gullstrand. [cited 2018-05-04]. Available from: http://www.ne.se/uppslagsverk/encyklopedi/lång/simulator

[5] Swedish Standards Institute, SS-ISO8855:2011, *Road vehicles - Vehicle dynamics and road-holding ability - Vocabulary*, Stockholm; 2012.

[6] Jacobson B, et al, *Vehicle Dynamics: Compendium for Course MMF062*, Gothenburg: Chalmers University of Technology; 2016.

[7] Smith C, *TUNE TO WIN: The art and science of a race car development and tuning*, Fallbrook, CA: Aero Publishers; 1978.

[8] Veen J. *An analytical approach to dynamic irregular tyre wear*[master's thesis on the internet]. Eindhoven: TU Eindhoven; 2007 [2018-05-07]. Available from: http://www.mate.tue.nl/mate/pdfs/8196.pdf

[9] Wright C. Book: The Contact Patch [Internet] [cited 2018-05-07]. Available from: http://the-contact-patch.com

[10] Cruden, Car physics [Internet]. Amsterdam: Cruden; [January 21, 2014; 2018-05-11]. Available from: http://racer.nl/reference/carphys.htm

[11] Happian-Smith J. *Modern Vehicle Design*. Oxford: Butterworth-Heinemann; 2001.

[12] Dixon J. C, *Suspension Geometry and Computation*, Wiley: West Sussex; 2009.

[13] W. F. Milliken, D. L. Milliken, *Race Car Vehicle Dynamics*, Warrendale, PA, USA: 1995.

[14] Zedaro. Zedaro zRack 358 User Manual [pamphlet on the internet]. Kitchener, On: Zedaro; 2016[cited 2018-05-13]. Available from: https://cdn.shopify.com/s/files/1/0698/1889/files/Zedaro_zRack_358_User-_Manual_20161115.pdf

[15] Segers J, *Analysis Techniques for Racecar Data Acquisition*, Second Edition, Warrendale, PA: SAE International; 2014.

[16] OptimumG. OptimumT Tutorial 3 [Internet]. Cennetanial, CO: OptimumG; [cited 2018-05-13]. Available from: http://www.optimumg.com/docs/OptimumT_Tutorial3.pdf

[17] Wittek, AM, Richter HC, Łazarz B, *STABILIZER BARS: Part 1. CALCULATIONS AND CONSTRUCTION*, Katowice: Silesian University of Technology; 2010

[18] VOLVO CAR CORPORATION INSTALLS ACTIVE SEAT AND ACTIVE BELTS FROM VI-GRADE ON DIM DRIVING SIMULATOR. 2017, 13th April [2018-05-04]. I/In: VI-grade engineering software & services NEWS. Marburg VI-grade engineering software and services; Available from: https://www.vi-grade.com/en/about/news/volvo-car-corporation-installs-active-seat-and-active-belts-from-vi-grade-on-dim-driving-simulator_34/

A

Appendix A

Questionaire

1. Steering wheel torque

Too little Too much

Comment:

2. Front grip when turning

Too little Too much

Comment:

3. Rear grip when turning

Too little Too much

Comment:

4. Front grip under braking

Too little Too much

Comment:

5. Front grip under hard braking

Too little Too much

Comment:

6. Rear grip under braking

Too little Too much

Comment:

7. Rear grip under hard braking

Too little Too much

Comment:

8. Rear grip when accelerating

Too little Too much

Comment:

9. Acceleration responsiveness

Too little Too much

Comment:

10. Steering wheel responsiveness

Too little Too much

Comment:

11. Braking responsiveness

Too little Too much

Comment:

12. Hard braking responsiveness

Too little Too much

Comment:

13. High speed stability

Too little Too much

Comment:

14. Low speed stability

Too little Too much

Comment:

15. Body roll

Too little Too much

Comment:

16. Body dive

Too little Too much

Comment:

17. Body squat

Too little Too much

Comment:

General comments:

B

Parameters in Panthera

This table presents some of the parameters entered in Panthera that were of importance for this work. Not all parameters are listed, please refer to the car.ini for further reading.

Suspension parameters defined per axle		
y, z	m	Location of upper end of suspension with relation to the null point.
restlen	m	Actually the free length of the spring. Acts as origin for all geometry effects.
minlen	m	Minimum length for suspension travel, defines where the bump stop is located.
maxlen	m	Maximum length for suspension travel, defines where the rebound stop is located.
k	N/m	Spring rate with null point in restlen.
damper_curve	text	Location of a .crv file containing a look-up table for the damper.
camber_change_per_m	rad/m	Bump camber, origin is at restlen.
caster_offset	m	Almost caster offset at ground, needs to account for caster angle.
anti_pitch	-	For the front this is the amount of anti-dive. For the rear this is the amount of anti-squat. Given as a proportion.
roll_center x, y, z	m	Static roll center location with relation to x and z of null point, but y with relation to the null point.

Suspension parameters defined per corner		
x	m	Location of upper end of suspension with relation to the null point.
camber_change_steering	rad/rad	Camber change due to steering, normally opposite signs on each wheel of an axle. Origin at restlen.
toe_change_per_m	rad/m	Bump steer, origin at restlen. Normally different signs on each wheel of an axle due to toe definition
susp_y_change_per_rad	m/rad	Steer jacking, how much the wheel is pushed up per radian of steering. Normally different signs on each wheel of an axle.
kingpin_offset	m	Almost kingpin offset at ground, needs to account for kingpin angle. Normally different signs on each wheel of an axle.
Anti roll bar		
k	N/m	Force at the wheel as a result of difference in wheel position.
Wheel parameters defined per axle		
x,y,z	m	Position of contact patch center with relation to bottom end of suspension plus radius. Normally leave this at 0.
mass	kg	Unsprung mass for each corner.
inertia	$kg \cdot m^2$	Inertia of the wheel around the spin axis.
radius	m	Unloaded radius of the wheel.
width	m	Width of the wheel.
camber	∘	Camber in degrees, defined according to[5].
lock	∘	Max steer lock, defines the steering ratio together with steering wheel lock.
ackerman	-	Not actual ackermann factor, but degree of innerwheel turn per outerwheel turn.
max_braking	Nm	Amount of braking torque on full pedal travel.
braking_factor	-	Scaling of max_braking. Should be used for brake balance according to documentation but is not correctly defined for this use.
rolling_coeff	-	Coefficient representing the rolling resistance
contact_patch_width	m	Width of the tire contact patch
contact_patch_length	m	Length of the tire contact patch
tire_rate	N/m	Vertical tire spring rate

Wheel parameters defined per corner		
toe	∘	Toe angle. Positive sign is always counter-clockwise direction.
Aerodynamic parameters defined on body		
center	m m m	Vector defining the CoP of the body. Relative to null point in racer coordinates.
cx	-	The drag coefficient
area	m^2	Frontal area
Aerodynamic parameters defined per wing		
span	m	The span length
cord	m	The cord length
coeff_drag	-	The drag coefficient
coeff_down	-	The down coefficient. Notice it is down and not lift
center	m m m	Vector defining the CoP of the wing. Relative to null point in racer coordinates.
angle	∘	Angle of Attack
angle_offset	∘	Offset value of the angle
Engine parameters		
mass	kg	Mass of the engine, must bu subtracted from body mass if implemented here.
max_rpm	RPM	Limit for maximum rpm.
curve_torque	-	Normalized torque curve.
max_torque	Nm	The maximum torque achieved by the engine. Is multiplied with the torque curve to get the torque at the certain RPM.
To be specified for each gear		
ratio	-	Gearing ratio.
inertia	kg·m^2	Gearing inertia.
Pacejka parameters		
optimal_slipratio	-	Optimal slip ratio
optimal_slipangle	rad	Optimal slip angle
relaxation_length_lat	-	Lateral relaxation length
relaxation_length_long	-	Longitudinal relaxation length
damping_speed	m/s	Damping lateral and longitudinal speed
damping_coefficient_lat	-	Lateral damping coefficient
damping_coefficient_long	-	Longitudinal damping coefficient

C

Tyre fitting curves

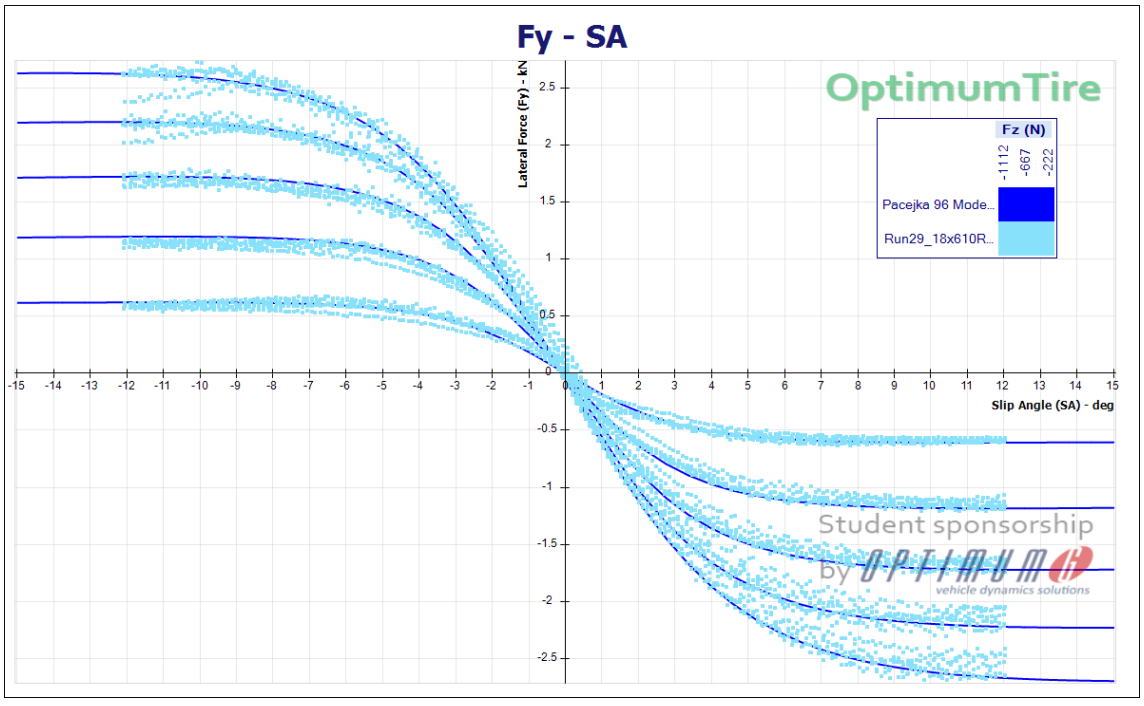

Figure C.1: Raw data light blue and curve fit dark blue at different loads

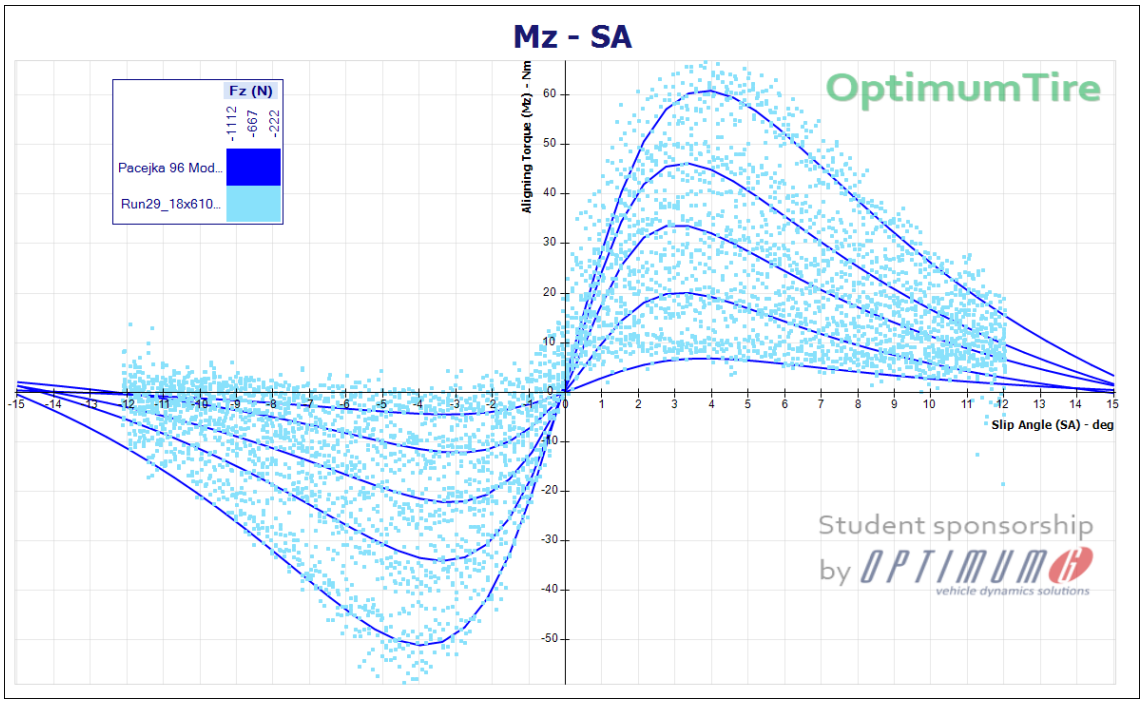

Figure C.2: Raw data light blue and curve fit dark blue at different loads

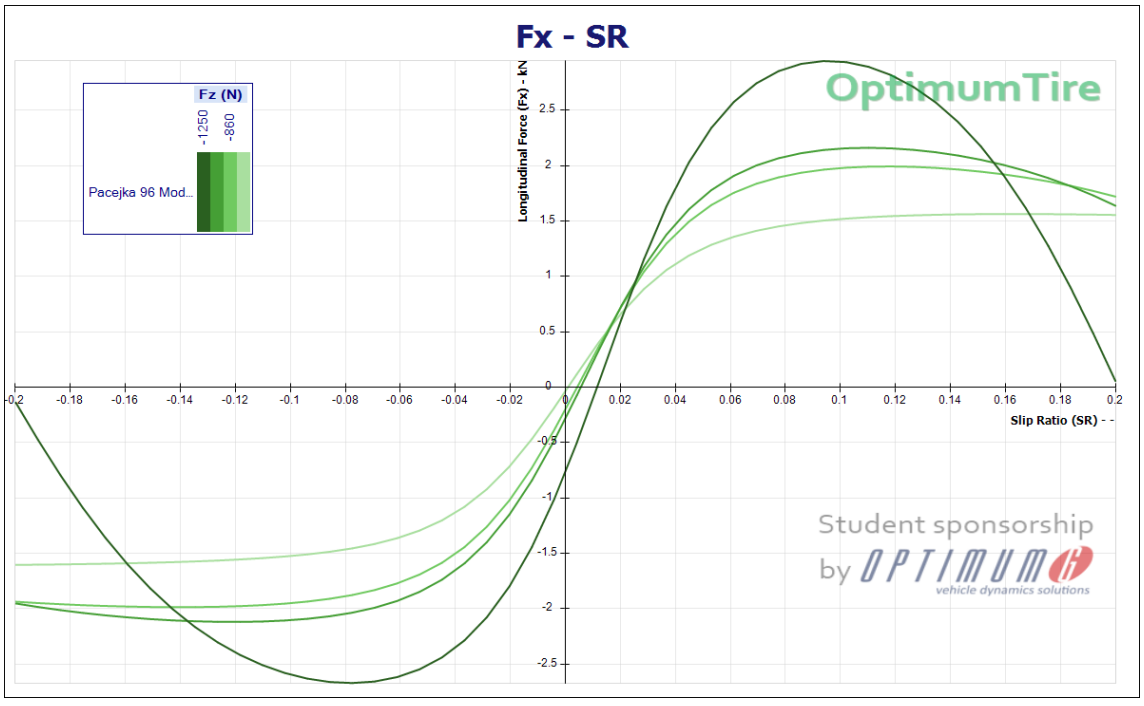

Figure C.3: Longitudinal force versus Slip Ratio at specified load cases

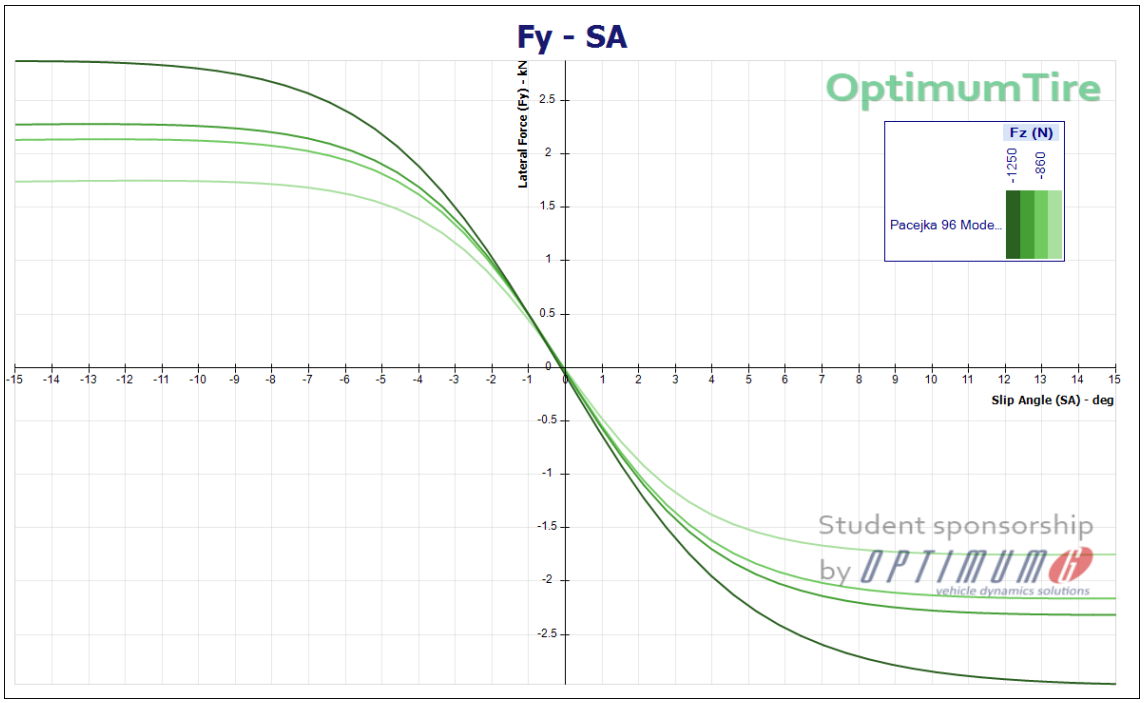

Figure C.4: Lateral force versus Slip Angle at specified load cases

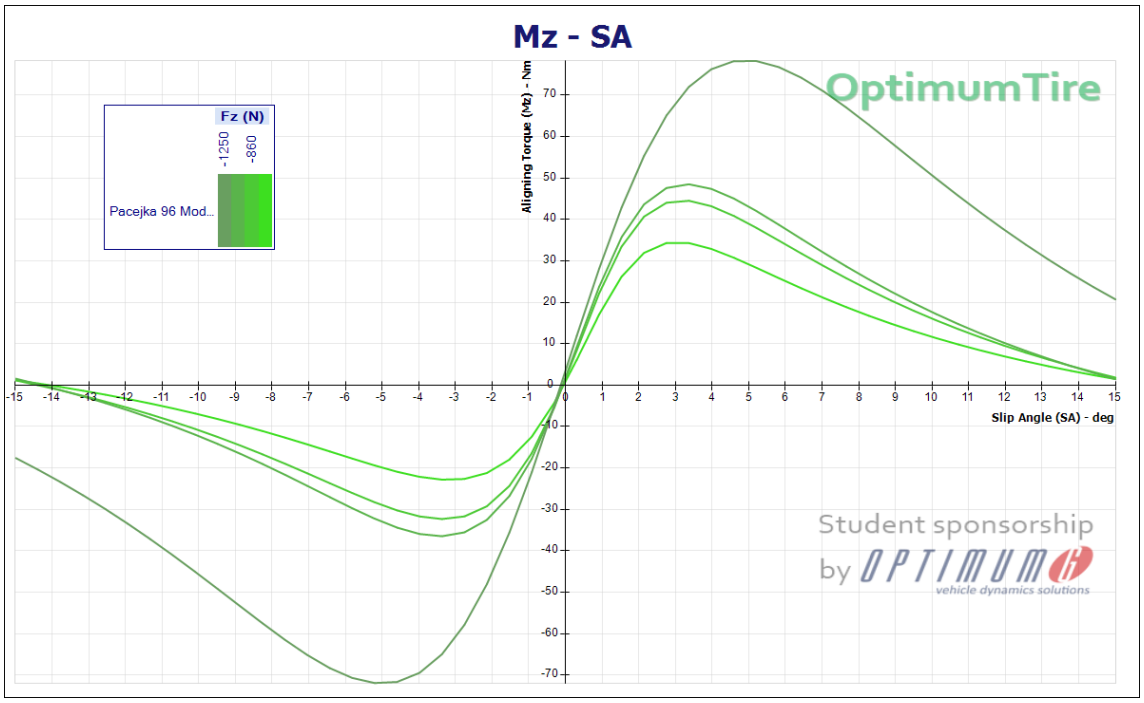

Figure C.5: Self Aligning Torque versus Slip Angle at specified load cases

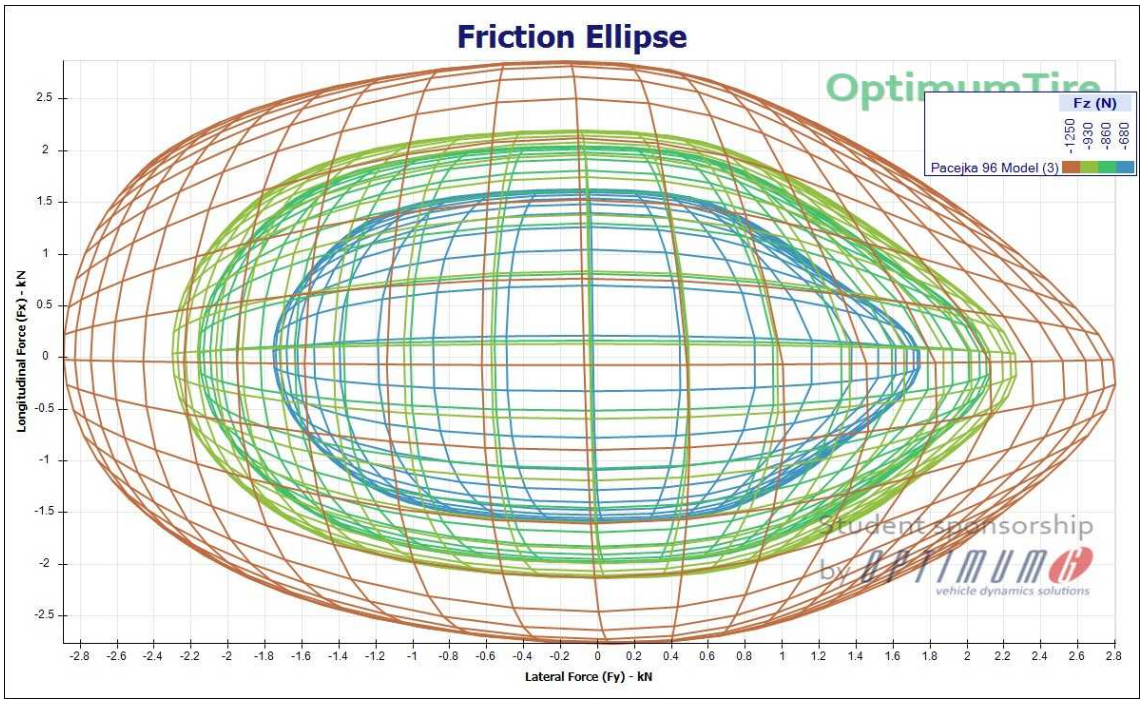

Figure C.6: Friction ellipse at specified load cases

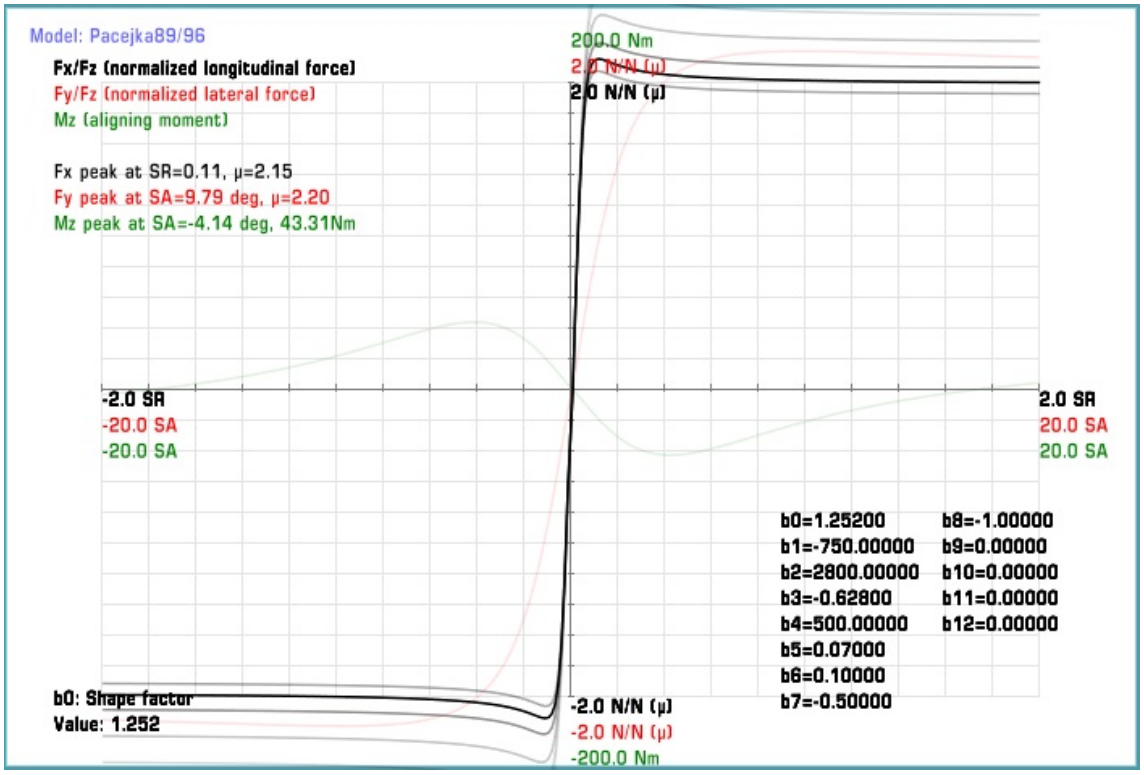

Figure C.7: Normalized longitudinal force versus Slip Ratio at specified RMS load for final Panthera tire model

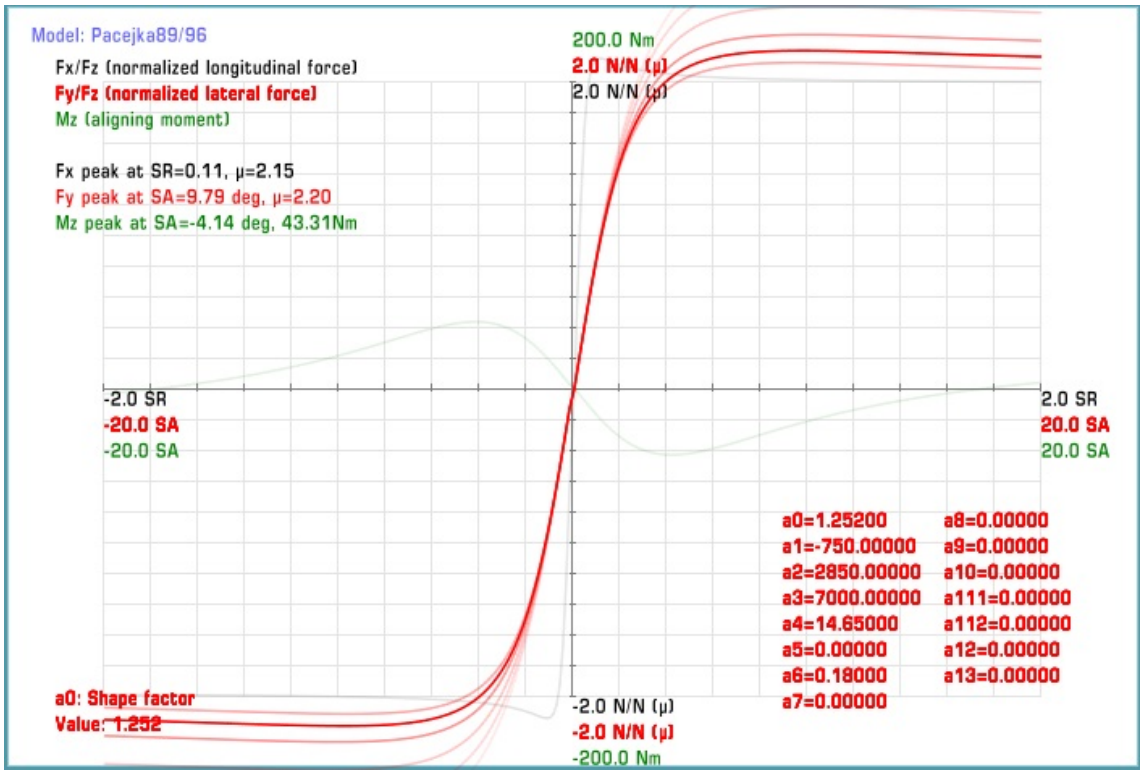

Figure C.8: Normalized lateral force versus Slip Angle at specified RMS load for final Panthera tire model

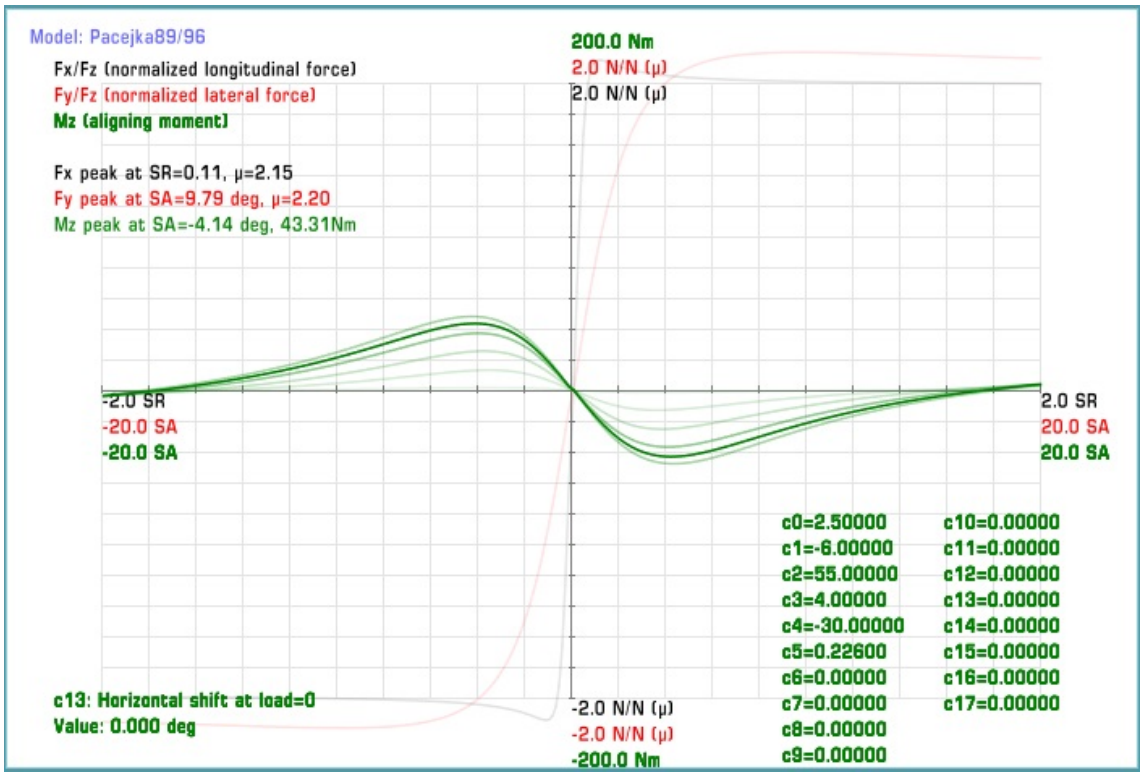

Figure C.9: Self Aligning Moment versus Slip Angle at specified RMS load for final Panthera tire model